Modified Equivalent Circuit

for Organic Solar Cells

by

Nazmul Hossain

A Thesis Presented in Partial Fulfillment
of the Requirements for the Degree
Master of Science

Approved July 2015 by the
Graduate Supervisory Committee:

Terry Alford, Chair
David Theodore
Stephen Krause

ARIZONA STATE UNIVERSITY

August 2015

ABSTRACT

In this work a newly fabricated organic solar cell based on a composite of fullerene derivative [6,6]-phenyl-C61 butyric acid methyl ester (PCBM) and regioregular poly (3-hexylthiophene) (P3HT) with an added interfacial layer of AgOx in between the PEDOT:PSS layer and the ITO layer is investigated. Previous equivalent circuit models are discussed and an equivalent circuit model is proposed for the fabricated device. Incorporation of the AgOx interfacial layer shows an increase in fill factor (by 33%) and power conversion efficiency (by 28%). Moreover proper correlation has been achieved between the experimental and simulated I-V plots. The simulation shows that device characteristics can be explained with accuracy by the proposed model.

DEDICATION

For my Parents and Wakil Uncle.

ACKNOWLEDGMENTS

I want to thank Prof. Dr. T.L.Alford who made it possible for me to work in his research group with all its benefits where I could learn so much not only about science but also life in general.

I am particularly indebted to Mr. Sayantan Das for his patience when explaning organic chemistry to me and pointing out which molecules could be synthesizes (and how!). I want to note that, unlike all other results described in this thesis- the experimental part in chapter 5 was carried out by Mr. Saysntan Das. However, the term “we” is used throughout the text to underline the fact that every single result of the author’s work as presented in this thesis was only possible because of the provision of equipment, materials and scientific input from others.

TABLE OF CONTENTS

Page

CHAPTER Page

CHAPTER Page

CHAPTER Page

LIST OF TABLES

LIST OF FIGURES

CHAPTER 1

BACKGROUND AND INTRODUCTION

The Combustion of Fossil Fuels

The economic prosperity and the technological development are the key challenges for the world herself. And Energy plays the most important roles for this issue[1]. Actually, the living quality of the people of a country completely depends on the energy storage of that country. The economy and the population are the vital factors for which the demand of energy has been increasing for last few decades. So, the energy issue is the burning question for the 21^{st} century[2]. In today's world, fossil fuels (gas, coal, oil *etc*.) are used extensively for cooling-heating, cooking and operating industrial as well as home appliances.

But, this energy sources are offensive to the environment as they produce huge carbon-dioxide (CO_2) during the burning period which causes to deplete the ozone layer at atmosphere that influences the green house effects more. Every year by burning fossil fuel about 20.10^{12}kg of carbon dioxide are put into the atmosphere. It is also responsible for global warming[3]. Since the late 19^{th} century the global mean surface temperature and the global sea level has increased by 0.3-0.6^{o}C and 10-25cm respectively [12]. These changes have already increased the number of natural disasters [13] and are likely to have devastating effects for human and other life forms all abound the world.

To protect the ozone layer, there are some steps taken by the different nations. For example, The Vienna Convention (1985), The Montreal protocol (1987) and the Kyoto protocol (1998) have suggested many rules and regulations to protect the ozone layer.

Recently, the NASA investigated that about an area of 28,300,000 km^2 of hole is found in ozone layer in two earth poles[4]. Hence, the European Commission (EC) Regulation

Table 1

The total solar radiations during the year of 2006 at Belgrade [10].

Months	Radiation (W/m^2)		Air Temperature (°C)
	Mean irradiance of global radiation	Mean irradiance of diffuse radiation	
January	50	30	0
February	100	50	3
March	150	75	6
April	200	100	12
May	225	120	17
June	250	125	19
July	270	120	21
August	225	100	20
September	200	75	18
October	120	60	12
November	70	40	7
December	50	25	2

2037/2000 implemented some rules to control the use of ozone depleting materials. And, this can be assumed that within 2015 all HCFCs will be banned[5]. Then, the eyes go to search for alternative energy source to protect the earth before the ending of conventional resources. And, renewable energy draws the best attention among the alternatives[3].

Renewable Energy Sources

The energy which is natural, inexhaustible and naturally replenished can be termed as "Renewable Energy". The hydropower, the geothermal, the tidal, the wind, the wave, the biomass and the solar are the most available forms of renewable energy[2]. There are so many renewable energy systems used all over the world. In Germany and Netherlands, there are some wind turbine power plants installed for producing electricity. There are some countries in Asia like Malaysia and India; they have many wind turbine systems. In Bangladesh, they are also using tidal energy by installing some hydro power plants. In the north-west of Iran, there is some geothermal energy produced by the mineral material[6]. About 70% of factories are using the geothermal energy in the Iceland. This vast usage of renewable energy indicates that it is more cost effective and totally pollution free than fossil fuels[3]. And among all these forms of renewable energies, solar energy is becoming more favorite day by day for its environmentally friendly and naturally availability characteristics[2].

Solar Energy

In the recent years, the scientists have given more eyes to the solar energy to handle the energy shortage issues all over the world[7]. To receive or hold the solar power, there are so many technologies invented which include the food drying, the heating, the cooking, the cooling and producing electric power[1].

In many countries of the world, solar energy is being accepted enormously for having low price (after installation), cleanliness and naturally availability of it. For example, in 2001, Sweden installed a solar power plant for commercial purposes. Besides, Turanjanin *et al.*[10] made a comparative study on solar radiation during a year of 2006 in Belgrade which is summarized in the Table 1.

The earth receives the solar power from the sun by the electromagnetic radiation technique. A thermonuclear reaction is performed inside the core of the sun and thus the solar energy is produced. The light, generated from the sun, is ultraviolet, visible and infrared. Actually, except the nuclear, the geothermal and the tidal energy, all of the existing energy resources are completely dependent on the Sun[8]. The surface of earth is receiving a huge amount of solar energy in every single moment. For example, a case study showed that the mean solar radiation is 1368 W/m^2[9]. Therefore, if we consider the surface area of 1.275×10^{14} m^2 and the radius of earth is 6372 km, then the total radiation from the sun to the earth will be 1.74×10^{17}W[6].

According to the solar system, the solar energy has two different classifications. First of all, the energy can be used as thermally driven system with solar collector which is called solar thermal power. On the other hand, the solar power can be used to produce the electricity by means of solar photovoltaic (PV) panel. Actually, the panel consists of several solar PV arrays. However, the system sometimes works with standalone and sometimes with other renewable or conventional power systems which is called the PV hybrid system[11].

PV System Standalone

In today's world, about 1.64 billion people are outside the coverage of electricity of which most of the people live in the rural areas where grid connections are not available [7]. For example, about 80% of the people in Asia and Africa live in the rural side. Sometimes, they produce electricity by operating diesel generators. But, it has high maintenance and operational cost. Again, there are some remote areas (especially in hills and forests), where the establishment of grid connection as well as the fuel transportation are very difficult; in such case solar PV system is the best alternative energy system to supply the electricity[12-14].

A photovoltaic cell is made of solid-state-semiconductor device (same as computer chips) which is capable to convert the sun light into electrical energy. The PV cells are used widely in various applications in recent world. In the calculators and the wrist watches, the power supplier is nothing but the small PV cells. Moreover, it is also widely used in commercial and domestic purposes to operate the fans, the heater, the lights, the motor, the air-conditioner, the refrigerators etc.[15]. The fig 1 shows a comparative representation about the development of solar PV system among USA, Japan, European countries as well as the rest part of the World. Most of the electrically driven equipment's are designed such way that the operating power should be alternating current, but the output of solar PV cell is direct current (DC).

Inorganic Solar Cells

At present, solar cells are used as small scale devices such as pocket calculators, water pumps and roof top solar panels, which are fabricated from inorganic semiconductor such as multi-crystalline and mono crystalline silicon. These cells are capable of harvesting up

to 24% [14] of the incoming solar energy which is almost same as the theoretically predicted upper limit of 30% [15]. This illustrates that technology that will allow low fabrication costs but somewhat higher conversion efficiencies – is desired now. Reducing the amount of silicon would be one approach to do that. But the production of these conventional solar cells still requires numerous lithographic steps and many energy intensive processes at high vacuum conditions and high temperatures (400-1400^{o}C), which lead to very high manufacturing costs [16].

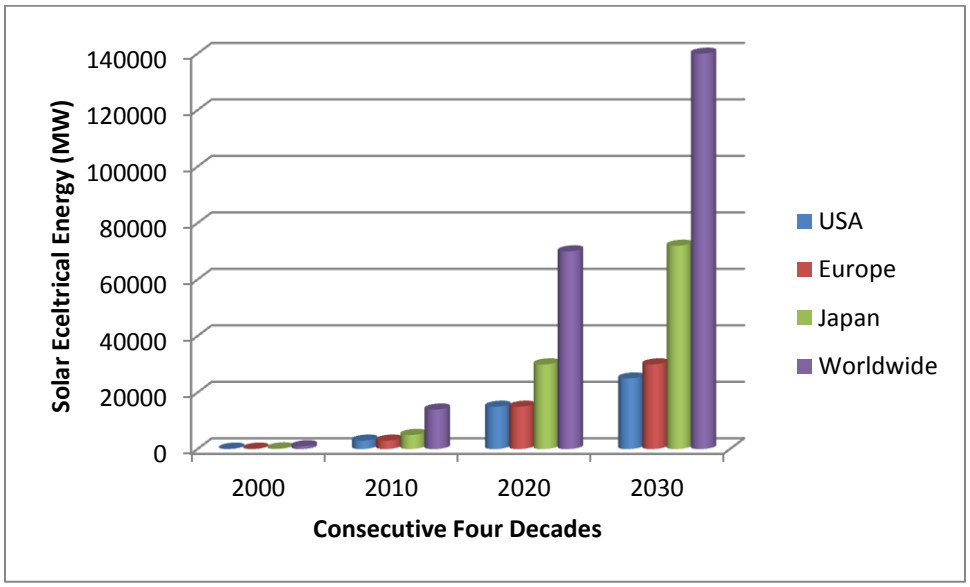

Fig 1: PV based solar electrical energy production for four decades all over the World.[15]

Organic Solar Cells

The fabrication of organic solar cells requires less production energy and effort as organic semiconductors are simple to process at much lower temperature than the inorganic cells [17].

Due to the molecular nature of the organic materials, organic solar cells are easy to manufacture compared to silicon cells. Molecules are can be used with thin film substrates that are 1,000 times thinner than silicon cells. And as mentioned before, this fact by itself can reduce the cost production significantly.

Organic solar cell presents versatility in their production methods because organic materials that are used for fabrication process are highly compatible with a wide range of substrates. These methods include high throughput printing techniques, solution processes (inks or paints), roll-to-roll technology and many more, that enable organic solar cells to cover large thin film surfaces easily and cost-effectively. All these methods have low energy and temperature demands compared to conventional silicon cells and can reduce cost by a factor of 10 or 20.

The amount of energy consumed to manufacture an organic solar cell is less than the amount of energy required for conventional inorganic cells [16]. Consequently, the energy conversion efficiency doesn't have to be as high as the conventional cell's efficiency. An extensive use of organic solar cells could contribute to the increased use of solar power globally and make renewable energy sources friendlier to the average consumer.

Electro-chemical solar cells using an organic dye in conjunction with titanium dioxide and a liquid electrolyte [17] has a power efficiency more than 6% and are about to enter the commercial market. Their production costs are relatively low.

The liquid electrolyte generates problems with sealing against air which is a disadvantage of electro-chemical cells when compared to polymeric photovoltaic cells.

Overview of the Thesis

The main task of this thesis was to fabricate and investigate the characteristic of newly developed AgOx based organic solar cell which may lead to the power conversion efficiency. A modified equivalent circuit model was proposed to explain the characteristic of the solar cells. In this thesis we fabricated an organic solar cell with an added AgOx interfacial layer. Improved efficiency and fill factor is shown by the device. An equivalent circuit approach to explain the characteristic of the device is proposed.

The thesis structure is in the following way:

In Chapter 2, basics physics of organic solar cells are discussed. First, overviews of the atomic organic molecular crystals that are used to fabricate the solar cells are given. Next, the charge carrier transport process will be discussed. Due to the polaronic nature of charge carriers the transport mechanism in organic solar cells are much more complex than inorganic solar cells. In organic solar cells very strongly bound Frenkel excitons are created after light absorption. Several mechanisms by which an exciton can travel will be discussed too. Next, the optical properties of organic solar cells and different photovoltaic parameters will be discussed. Finally, basic principle of doping and device architecture of organic solar cells will be discussed.

In Chapter 3, fabrication process technology for organic solar cells is reviewed. The principle of device fabrication, preparing substrate, spin-coating, thermal vacuum evapotaion, is briefly explained. Explanation of current-voltage (I-V) measurement setup is also given. Furthermore, ultraviolet and X-ray photo electron spectroscopy, material purification, electrode materials which were used for the fabrication are also discussed in this chapter.

In Chapter 4, basics of equivalent circuit approach to understand and explain the behavior of the organic solar cells are discussed. Different parameters of the an equivalent circuit are discussed and explained. Finally, equations to measure the short circuit current (I_{SC}) and open circuit voltage V_{OC} will be deduced.

In Chapter 5, the basic characteristics of the fabricated device are discussed. Results for power conversion efficiency, increase of fill factor are given. A modified equivalent circuit model to explain the behavior of the fabricated device is explained. Finally, the I-V curve resemblance for the simulated and experimental data is shown and discussed to support the modified equivalent circuit model of the solar cell.

CHAPTER 2

ORGANIC SOLAR CELLS

Overview

To convert solar light into electric power it is required to generate both positive and negative charges and a driving force that can push these charges through an external electric circuit [18]. Any electric device such as a computer monitor or a water pump that is connected to the external electric circuit can utilize the converted solar energy. Hence, a solar cell may be described as a solar-light driven electron pump: where the maximum height the electrons can be pumped is equal to the maximum voltage developed by the solar cell. The pump rate determines the maximum current.

Suppose the solar light driven electron pump can promote 100 electrons/s from the valence band (VB) into the conduction band (CB), then the maximum possible continuous current of electron that can flow through the external circuit is 100 electron/s. If the current is reduced by *e.g.* a load resistor to 80 electrons/s, the remaining 20 electrons/s will drop back into the VB before they can leave the device. In real semiconductors, these leakage currents are simply realized by the *recombination* of the photo-excited charge carriers or using our analogy: the"pumped" electrons drop back into their VB. These leakage currents are typically caused by defects or other deviations from the ideal semiconductor structure which gives rise to the appearance of allowed energy levels *within* the bandgap [19]. Only if there are virtually no such defects, *radiative* recombination will remain the only decay channel since it does not require the existence of mid-gap levels but can occur directly from band to band.

General Properties of Organic Semiconductors

Organic materials have strong electron-phonon interaction which makes the photo physics different than the inorganic semiconductors [19]. The photo excitation does not automatically generate free charge carriers, bound electron-hole pairs (excitons). These excitons have a binding energy of about 0.4 eV [18-20]. To transport the charges through the film and collect them at the electrodes, these excitones need to be dissociated. For example, exciton can be split up at the interface between an electron-acceptor and an electron-donor semiconductor. The exciton dissociation depends on the interface area. The larger the interface is the more excitions are dissociated.

Typically the excitons have a diffusion range about 10 nm [21-24] which is smaller than the necessary thickness of the film to absorb the major portion of light. This makes it difficult to obtain certain conversation efficiency.

Fermi-level

The Fermi level in the semiconductors determines whether a blocking contact or Ohmic contact is formed at the interface. Whether the semiconductor is p-type or n-type is also determined by the Fermi level more accurately the position of the Fermi level. The material is called n-type conductor when the Fermi level is close to the CB otherwise it is called p-type conducting. The energetic position of the Fermi level (E_F) can be represented by the following relation:

for p-type semiconductors this is given by:

$$E_F = E_V - kT.\ln(\frac{N_V}{N_A}) \quad (1)$$

whereas, for n-type semiconductors the relation is given by

$$E_F = E_C - kT.\ln(\frac{N_C}{N_D}) \quad (2)$$

E_C and E_V represent the bottom edge of the CB and the top edge of the VB respectively [25]. N_C, is the effective density of states in the conduction band, N_V is the effective density of states in the valence band, N_D is the concentration of donors, and acceptor concentration is N_A

The concept of Fermi level does not apply when voltage is applied and/or semiconductor is illuminated. When the semiconductor is illuminated the increased concentration on electrons in the CB would shift E_F up while the higher concentrations of the VB will shift E_F down. As a result there are two separate Fermi levels. And they can be given by

$$E_{FP} = E_C + kT.\ln(\frac{N_V}{P}) \quad (3)$$

$$E_{FN} = E_C + kT.\ln(\frac{n}{N_C}) \quad (4)$$

where n and p denotes the concentration of electron and holes. And E_{FP} and E_{FN} are the quasi Fermi-levels.

Doping

In inorganic semiconductors introduction of dopant atoms provide free charge carriers at room temperature [26]. As a result the conductivity of the charge carrier increases. In organic semiconductors doping is introduced by foreign molecules. Another way to achieve doping is electro-chemical oxidation or reduction which is discussed later. Moreover, trapping changes the concentration of mobile charges. But in case of trapping there is no net increase of mobile charge carriers. So the conductivity is not increased. However, in practice upon exposure to oxygen the conductivity is increased.

Complexation with foreign molecules increases the concentration of mobile charge carriers and therefore the conductivity. These doping molecules do not diffuse or penetrate into another material since they are preferably large polymers. PANI with camphor-sulfonic acid or PEDOT with polystyrene sulphonic acid demonstrate this type of doping [25]. Organic semiconductors have very few mobile charges available in the dark. For this reason, extra mobile charges due to illumination can have a significant impact. [26].

Structural Properties of Organic Semiconductors

Materials

Polymers and low-molecular weight materials are the two major organic semiconductors [27]. In the molecules the p_z orbitals of sp^2 –hybridized C atoms form a conjugated p-electron system in both of these materials. The π bonding is much weaker than the σ bonds which are the backbones of the molecules. Therefore, for the conjugated molecules the π-π^* transitions are the lowest electronic excitations. Typically they have an energy gap between 1.5 and 3e.V. In the visible spectral range this leads to light emission or absorption. In general, the presence of electron donation or withdrawing groups and the conjugation length are the determining factors for the electronic properties of a molecule. For that reason, a wide range of possibilities are offered by organic chemistry to adjust the optoelectronic properties.

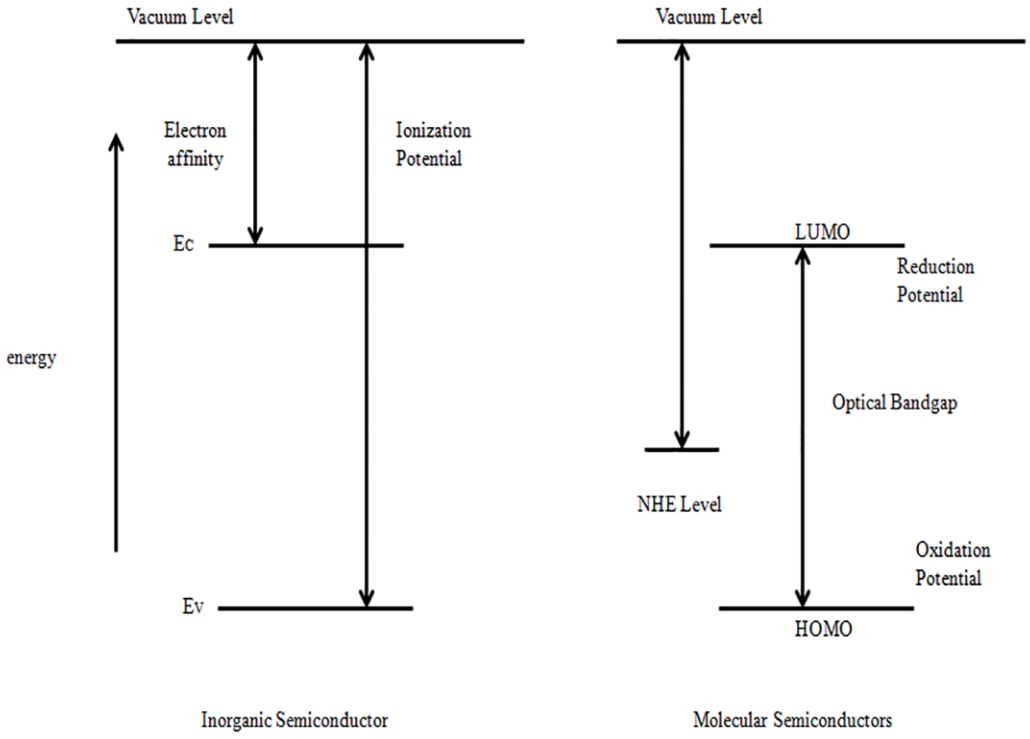

Fig 2: Energy level overview for inorganic and organic solar cells.

.

The process to fabricate thin films is the main difference between the two classes of materials. Conjugated polymers are processed by spin-coating or printing techniques whereas small molecules are usually processed by evaporation [29]. The processing cost of this solution is low, but they need soluble polymers. For example Poly [p-henylene vinylene] is hardly soluble. So, poly[2-methoxy-5-(3',7'-dimethyloctyloxy)-1,4-phenylene vinylene] is used to enhance the solubility of the polymer [28].

The energy levels of inorganic solar cells can be compared to the energy levels of organic solar cells. Fig. 2 shows the energy level diagram for organic and inorganic solar cells. In inorganic solar cells, to release an electron from the valence band to the vacuum level is

represented by the ionization potential. Electron can be released to vacuum in molecular materials form the highest occupied molecular orbital (HOMO). The energy involved in this process can be approximated from the relation: $E_{HOMO} \approx E_{NHE} - V_{OX}$, with E_{NHE} = -4.5 V *vs.* vac. In a similar manner the electron affinity can be estimated from the relation: $E_{LUMO} \approx E_{NHE} - V_{red}$. The difference between these two energy levels of molecules is the optical bandgap. Molecular materials having low ionization potential donate an electron and are represented as electron donors. And materials with high electron affinity are called electron acceptor who can easily take an electron. This is an intrinsic property of the compound.

Polarons and Polaron Excitons

In classical polar crystal the electrons attracts the nuclei resulting in a polarization while repulses the adjacent electrons. The mobility of the quasi-particles is decreased because of the polarization. The conjugated systems have neither pure polar nor pure covalent bonds [28]. In comparison to inorganic solids they exhibit a huge electron lattice coupling [29]. In conjugated systems polarons and polaron excitons are generated due to this strong electron-lattice coupling. Additional energy levels appear within the semiconductor bandgap which can identify the quasi particles [30]. Fig. 3 shows the energy level diagram for polarons. While travelling the polarons changes the nature of the bonds from σ to π via excitation. This leads to a more rigid structure in the excited state. In the following section a brief overview is on the differences between excitons in inorganic and organic solids is given:

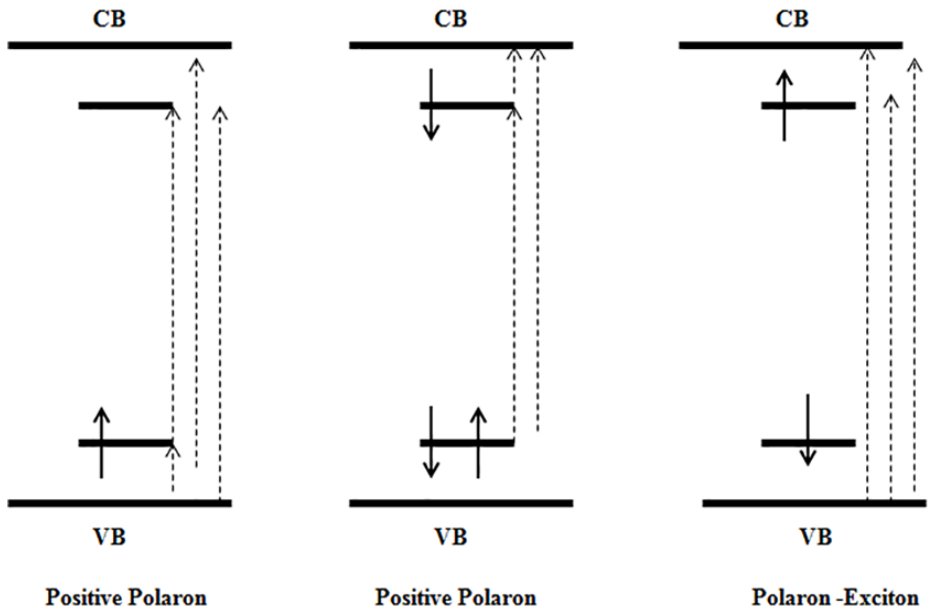

Fig.3: Energy levels for positive polaron, negative polaron, and polaron excitons. Dashed arrows represents possible intra gap transitions and solid arrows represents the spin orientation of electrons. [31]

In inorganic solar cells the excitons become important predominantly at lower temperature because of the binding energy E_b (typically 16meV) [31]. This energy can be reduced further if the excitons bind with defects. All of the excitons can occupy the lowest lying state. The free exciton gas can condense at high densities and low temperature to produce an electron-hole liquid phase [32].

In onganic semiconductors the binding energy of excitions range from a very small value (around 0.4eV) [18-20] to very high value (up to 0.95eV) [33]. As a result the excitons are separated from the conduction band (CB) and Valence band (VB). However, at room temperature a clear offset is still required in the D/A material between HOMO and

LUNO levels for the excitons to dissociate. There are different types of excitons. They are: [32]:

(i) Frenkel excitons,

(ii) Mott-Wannier exciton,

(iii) Charge transfer exciton,

(iv) Inter-chain exciton, and

(v) Intrachain exciton

In organic semiconductors there is another important excited species called "excimer". An excimer is only stable in the excited state [26, 34]. Therefore, it shows little vibronic structure in the emission spectrum.

Light Absorption

The absorption spectrum of photoactive organic layer should be sufficiently thick and should match the solar emission spectrum in order to collect the photons efficiently. The optical absorption coefficient (α) of organic materials is usually higher than the absorption coefficient of multicrystalline or crystalline silicon [35]. Approximately an optimal band-gap of 1.1 eV is needed for a single light absorbing medium based photovoltaic cell. An increase in the photocurrent can be expected by lowering the band gap of the organic material and harvesting more sunlight. Increasing the layer thickness often facilitates the light absorption but at the same time it hampers the charge transport. As a result of this the fill factor is lowered.

Exciton Transport

Excitons are formed due to light absorption and they should lead to the formation of free charge carriers [35]. However decay process such as radiative recombination, luminescence also take place at the same time. The reciprocal value of all radiative and non radiative decay rates together determines the exponential life time of excitons (τ_{EXC}). All excitons should reach the interface within this lifetime. The distance an exciton is able to cross in given by

$$L_{EXC} = \sqrt{\frac{D_{EXC}}{\tau_{EXC}}} \tag{5}$$

where D_{EXC} is the diffusion coefficient of the excitons. Typically the excitons lifetime τ_{EXC} is several nanoseconds at most, L_{EXC} is limited to 10mm. So only the excitons that are created within a distance of L_{EXC} from the interface will contribute to charge separation. From equation (5) we can see that increasing the diffusion coefficient will increase L_{EXC}. Increasing L_{EXC} means that each generated exciton is close to an interface.

Charge Separation

Conversion of solar light into electrical energy depends on the creation of charges from extions. Usually charges are created by photoinduced electron transfer in most organic solar cells. An additional input energy of an absorbed photon is given to transfer the electron from an electron donor (D) to an electron acceptor (A). Electron donor is a material with low electron affinity. And electron acceptor has high electron affinity. The force required to create charges from the excitons is the difference between both electron affinity levels. An exciton is dissociated at the D/A interface by creation of a charge

separation state. The charge-separation state consists of radical anion and cation of the acceptor and donor respectively [36].

$D+A+h\upsilon \rightarrow D^{*} + A \text{ (or } D + A^{*}) \rightarrow D^{*+} + A^{*+}$

Thermodynamically and kinetically the favorite pathway for the exciton should be the charge-separated state. Hence, it is important that the charge-separation state is generated by using the absorbed photon energy. Moreover, the charge-separated state has to be stable to migrate the photogenerated charges to the electron. To ensure this the recombination should be slowed down as much as possible. In a homojunction silicon semiconductor under illumination, electron flows from the p-type to the n-type semiconductor. In case of heterojunction under illumination, electron flows from D to A. Therefore, in analogy with silicon pn junction D layer is the p-type layer and A layer is the n-type layer.

Carrier Transport

Some organic materials that show semiconducting properties offer unique opportunities. But they have different functioning and behavior than inorganic semiconductor. Halogen doped perylene charge-transfer complexes were the first organic maerial to exhibit semiconducting behavior. In 1963 and 1965 Weiss discovered semi-conductive doped polymer [36, 37]. However, today this type of organic semiconductor is not typically used. Since most of the aromatic organic materials have extremely low intrinsic carrier, without proper doping their conductivities are extremely low [38]. In 1960 Pope and his colleagues developed and explored the charge transportation in these materials [39,40]. He worked with various acene crystals, such as naphthalene and anthracene, with highly efficient dark injection of charges [40]. His work was the beginning of the organic

electronics as it is known today [41]. Sufficient charge is injected by this charge injection. This can also be accomplished by field effect depletion, photoexcitation or chemical doping [42].

The molecular nature is one of the major differences between inorganic and organic semiconductors. The molecular orbitals of each molecule's play the role of conduction and valence bands [43]. They are analogous to the lowest unoccupied molecular orbital (LUMO) and highest occupied molecular orbital (HOMO) respectively. The band gap energy of organic materials is determined by the separation of these energy levels. The type of carrier injected into them determines whether they are considered n-type or p-type materials. Charge transport from one molecule to another is a hopping process in such localized systems. The relatively low mobilities of organic charge transport materials are increased by this localization and potential for scattering, collisions, and delays. Some undoped, high purity organic single crystals have shown band type transport but high conductivity has been shown by doped organic transport materials [40,42]. Although organic semiconductors have low mobilities and intrinsic carrier densities than inorganic semiconductors, they offer several advantages [44] including various possible structures, responsive to large area coverage, ease of synthetic modification, highly sensitive to chemical and biological agents.

In organic charge transport materials the charges quantum mechanically tunnel from one molecule to the other. The transport of charge is described as hopping [42]. This hopping process is like a series of redox chemical reactions where extra holes and electron are isolated as cations and anions respectively. This excess charge is transferred to a close neutral molecule by the ionized species. Under the influence of the external field this

helps to move the charge through the material even though the molecules remain stationary [43]. The relaxation energy λ and the transfer integral are the two major factors to facilitate such transport. The transfer integral is basically the overlap of the LUMO and HOMO levels. The hopping rate and the carrier mobility are proportional to the transfer integral. While changing the charged states molecules change their geometries, and this results reorganization energy λ. The reorganization energy is inversely proportional to the transfer process.

There are some factors that cannot be simulated to determine the hopping rate in a material. True reorganization energy is one of them. In organic solids charge transport involves the reorganization of electron clouds and possibly geometry of many molecules. These effects are the basis of polaronic theories of charge transport in organics [45]. However, impurities, many body effects, defects, transport pathways, and other complex issues make it difficult for quantitative prediction.

Despite all these difficulties in molecular-level simulations, there are a number of properties that helps to simulate the charge transport in organic materials accurately. First, in disordered organic materials the charge carrier mobility depends on the applied field. Thus the mobility is a function of the field. Second, carrier mobility depends on the temperature. Hopping is thermally activated and the mobility is proportional to the temperature. To overcome the barrier from energetic disorder additional thermal energy is provided. The Poole-Frenkel conduction formalism and an analogy to Arrhenius-like behavior can be shown to be applicable to explain organic charge transport materials for fields from 10^4 to 10^6 V/cm [46,47]. However, for this kind of measurement the accessible temperature range is limited. Bässler's Disorder formalism is the most notable

model to relate both the temperature and field dependence [48]. Substantial research has been done to show how the mobility increases with different compositions of species [49]. Trap control transport has shown good control over mobility.

In an organic molecular solid transport of holes or electron involves ionic molecular states. In order to create a hole, *e.g.,* an electron has to be removed out of a neutral molecule M to form a radical cation M^+. And then the electron can move from one molecule to another. Similarly, negatively charged radical ions M^- need to be formed to transport electron. These ionic states are stabilized by the polarization energy. Figure 3 shows the energy level schemes.

Due to the exciton binding energy, the single particle gap to create an uncorrelated electron-hole pair is higher than the optical gap between the ground state and the first excited singlet state. So, depending on degree of order, in organic semiconductors charge transport mechanism can be divided into two groups- band and hopping transport. At low temperature band transport is observed in highly purified molecular crystals.

Charge Collection

A transparent conductive oxide (TCO) like ITO or SnO_2:F on one side and metal conductor on the other side is used to collect the charge carriers at the electrode. Better performance can be achieved by developing special contact layers. For example at the TCO side a PEDOT:PSS layer is used and LiF layer at the metal contact.

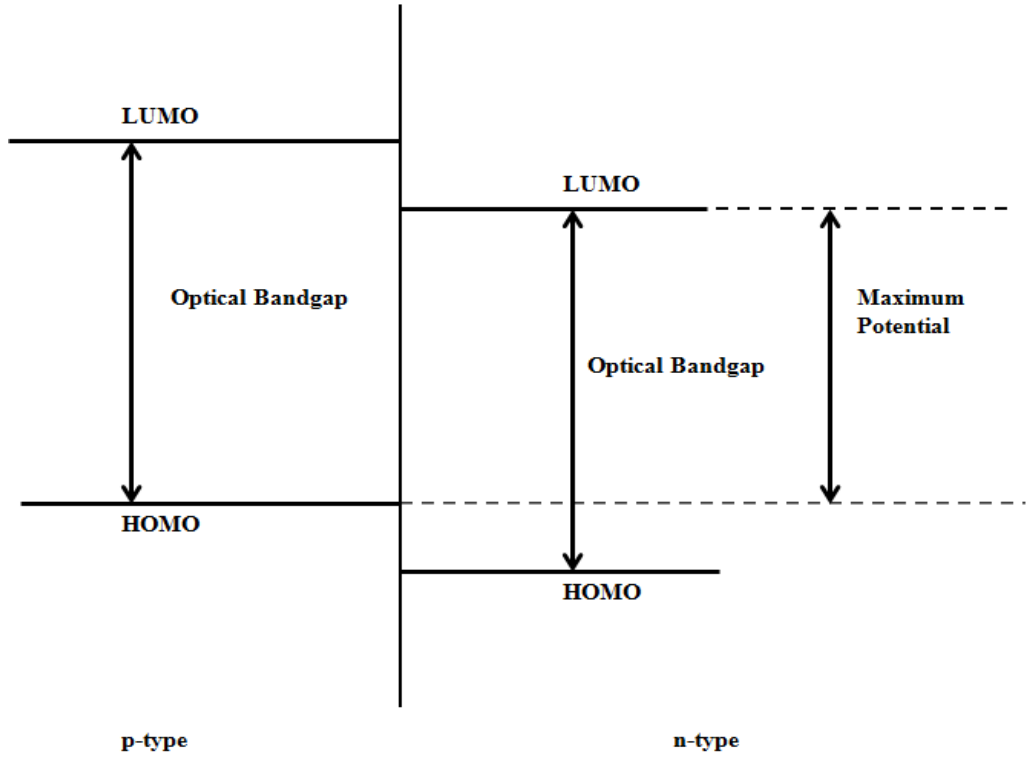

Fig. 4: Energy levels that determines the maximum potential generated by an exciton solar cell. LUMO offset energy level forms the driving force for the dissociation of excitons [48].

The electrostatic potential at the junction limits the open circuit voltage V_{OC} in inorganic solar cells. A reasonable voltage is measured for organic solar cells based on single molecular materials. In two molecular materials based organic solar cells optical excitation forms an exciton in one of the layers. Part of the photon energy is lost in the charge separation process to create an electron and a positive charge. Fig. 4 shows the maximum obtainable potential if there is no potential loss at the electrode.

Optical Properties of Organic Semiconductors

Organic semiconductors show some significant characteristics in comparison to their inorganic counterparts due to the weak electronic delocalization. One of them is the

presence of well-defined spin states. These spin states (singlet and triplet) has significant impact on the photophysics of these materials.

Usually in organic molecule the absorption of a photon leads to the first excited singlet state (S_1) form the ground state (S_0). Thereby the vibronic transitions within this manifold are determined by the Franck-Condon factor. The typical lifetimes of S_1 state are 1-10 ns. Thus there is a quick transition back to the S_0 ground state. From the triplet state (T_1) the excitation energy can be discharged either by non-radioactively or phosphorescence. But there is a small probability of intersystem crossing from excited singlet state to the triplet state. In pure atomic hydrocarbons triplet lifetimes are typically in millisecond range. That is why radiative decay is usually not observed at room temperature. Molecules incorporating with heavy atoms like Ir, Pt shortens the lifetime of the triplet significantly. Excitions are usually localized on one molecule. Therefore they have significant binding energy. To generate an independent pair of positive and negative charge carrier this binding energy has to be overcome.

Photovoltaic Parameters

The directly measurable parameters of a photovoltaic cell are the open circuit voltage V_{OC}, short circuit current I_{SC}, the fill factor FF. the power conversion efficiency η_p, and the incident photon to current efficiency IPCE. Fig. 5 shows the IV curves of a photovoltaic cell with and without illumination. Under illumination the current goes towards negative because of the photo generated current.

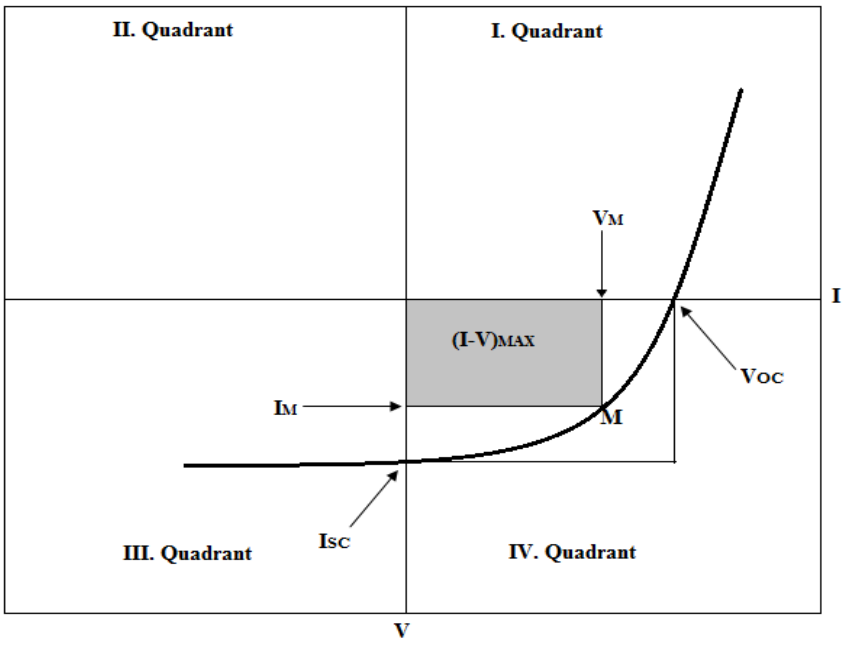

Fig. 5: Typical I-V characteristics curve of a photovoltaic device upon illumination. I_{SC} in the short circuit current, V_{OC} in the open circuit voltage, M is the maximum power point, I_M and V_M is the maximum current and voltage, and $(I\text{-}V)_{MAX}$ is the maximum power rectangle

Open Circuit Voltage

The voltage at which no current flows through the solar cell is called open circuit voltage V_{OC}. The open circuit voltage V_{OC} is strongly dependent on the energy difference ΔE between the HOMO and LUMO offset at the DA-interface of the Organic solar cell. Figure 4 shows the energy difference between the HOMO and LUMO offset. [50-53]. But the experimental values can differ from those inferred for some material systems. The difference can be the result of special electronic properties of the donor and acceptor at the DA-interface. So, a thorough understanding of the materials properties is required to develop a new OPV that will lead to a high V_{OC}.

Short-Circuit Current

The current at which there is no voltage (V = 0) is called the short circuit current I_{SC}. This is the current purely based on the photo generated charge carriers. Therefore, the spectral dependence of the charge carrier generation can be measured for monochromatic exposure.

Fill Factor

The maximum power point of a photovoltaic cell is determined by the maximum product of the voltage and current from the IV curve. And the maximum area is larger the more the IV curve resembles a rectangle with the area V_{OC} * I_{SC}. The ration between these two areas represents the quality of the IV curve and is called Fill Factor (FF).

$$FF = \frac{(IV)_{MAX}}{V_{OC} I_{SC}} \tag{6}$$

The series resistance of the cell strictly determines the fill factor. So the mobilities of charge carriers in the organic layers of the cell significantly determine the FF.

Incident Photon to Current Efficiency

The incident photon to current efficiency is defined as the ratio of the number of photo induced charge carriers N_{charge} which can be extracted from the solar cell to the number of incident photons N_{photon}. IPCE takes into account the losses due to scattering, reflection, and recombination; that's why it is smaller than the internal quantum efficiency. IPCE can be determined directly from the incident current density J_0 and the short circuit current I_{SC} [52].

$$IPCE = \frac{N_{\text{charge}}}{N_{\text{photon}}} = \frac{I_{SC} \cdot hc}{J_0 \cdot \lambda q} \tag{7}$$

where q is the single electron charge, c is the speed of light, λ is the wave length of the incident light and h is the Planck constant.

Power Conversion Efficiency

The photoexcited electrons can decrease its potential energy until they reaches the lowest lying level of CB (the LUMO). They do this by losing energy to phonons. The phonon energy dissipates into heat. This process is called thermalisation [52]. The semiconductor bandgap is often regarded as a measure for achievable voltage because of the thermalisation process. The higher the bandgap the higher the voltage can be.

A low bandgap material can absorb more photons. Therefore, the photocurrent increases with the increasing number of photogenerated charge carriers. The lower the bandgap, the higher the photocurrent is. So there must be a optimal bandgap for maximum efficiency under a given illumination. Shockley and Queisser were the first to calculate the maximum efficiency. For the calculation they only assumed the radiative recombination and the solar radiation on earth. Figure 5 shows the maximum power efficiency point in the current versus applied voltage graph. A high load resistance reduces the current flux. So, the charges need more time to get out of the semiconductor. Therefore, there are more recombination and the extracted external current decreases. This behavior is shown in the IV quadrant of the figure.

Thus form the IV curve- the maximum power is the maximum product of the voltage and the current. And it is given by the following relation:

$$P_{MAX} = (IV)_{MAX} = V_{OC} \cdot I_{SC} \cdot FF \tag{8}$$

Higher *FF* ensures higher electric power that can be extracted. And the IV characteristic resembles a constant current source with a maximum voltage. The current/voltage point

(V_M, I_M) that gives the largest power rectangle is called the maximum power point. So the load connected to the output will be able to use the maximum power output only if its supply voltage is around V_M. If the supply voltage is less than the maximum voltage, power would be wasted in heating the series resistor. If it is greater than the supply voltage, power would be wasted by increased current losses through shunt resistance and the ideal diode.

Therefore, to determine the power conversion efficiency η the maximum output power P_{max} has to be considered in terms of the incident light power P_{light}. So the maximum power conversion efficiency is given by-

$$\eta(\lambda) \equiv I_{SC}(\lambda) \cdot V_{OC}(\lambda) \cdot \frac{FF(\lambda)}{P_{light}} \tag{9}$$

where, λ is the wavelength. The power conversion efficiency is wavelength and intensity dependence [28,54]. Hence it is only meaningful for a certain spectral distribution and intensity. The most common standard solar radiation is the AM (air mass) 1.5 spectrum.

Organic Semiconductor Devices and Device Architectures

The current through a material on a macroscopic level is given by the carrier drift velocity v, the charge carrier density n. The drift velocity can be expressed in terms of the mobility μ and the electric field F. Equation (10) shows the relationship,

$$j = env = en\mu F \tag{10}$$

In organic semiconductors there is not a linear relationship between the current density j and the electric field F. From equation (1) we can see the current density is also dependent on the mobility and the carrier density n. So, it is enlightening to compare

these parameters for inorganic and organic semiconductors and find out different ways to control them.

As we have already discussed that the mobility in organic solar cells depends on the degree of order and the purity and therefore on the preparation and the growth condition. In molecular crystals in can reach to a value of 1-10 cm^2/Vs. But they can be as low as 10^{-5} cm^2/Vs in amorphous materials.

In a semiconductor with an energy gap E_g and an effective density of states N_0, the intrinsic carrier density is given by

$$n_i = N_0 \exp(\frac{-E_g}{2kT}) \tag{11}$$

Taking a typical value of E_g = 2.5eV and N_o =10^{21} cm^{-3} gives a hypothetical value of 1cm^{-3} for the carrier density at room temperature. This is unattainable due to impurities. The corresponding value of carrier density for Si is $10^{10}cm^{-3}$ (with $E_{g=}$1.12eV and N_0= $10^{19}cm^{-3}$). This shows that pure organic semiconductors have extremely low conductivity. Different approaches have been applied to overcome this limitation. They are as followed:

(i) photogeneration of carriers,

(ii) (electro-)chemical doping,

(iii) Field-effect doping, and

(iv) carrier injection from contacts.

These approaches are discussed briefly in the next section

(i) Organic photo-voltaic cells (OPVCs) are one of the most important device applications of organic semiconductors. But their large exciton binding energy

presents difficulties in OPVCs. This is because large exciton binding energy prohibits efficient exciton dissociation. This issue can be overcome by using photoinduced charge transfer layer between the donor and the acceptor [55]. OPVCs use the bulk-heterojunction concept of adding donor and acceptor in one single layer device due to the short exciton diffusion length. It as also challenging to achieve sufficient life time for OPVCs under ambient conditions [56].

(ii) One of the keys for success of organic semiconductor microelectronics is controlled doping. Ion implantation doping showed promises for organic semiconductors. But due to the need for sophisticated equipment and concomitant ion beam damages this method was not suitable enough for organic semiconductor devices. There are some other doping techniques which have been successfully applied. One of them is electro-chemical doping, which is basically chemical doping by adding strong electron donors and acceptors [57,58]. But there is a high risk of unintentional doping of organic materials during synthesis, and in many cases ambient oxygen cn cause p-type doping. For this reasons controlled doping needs to be further studied.

(iii) In organic field-effect transistors (OFETs) the charge carrier density in between source and drain channel can be controlled my controlling the gate voltage [59,60]. In the saturation and in the linear region the drain current in then given by equation (2) and (3) respectively,

$$I_D = \frac{w}{L} \cdot C_i \mu (V_G - V_T)^2 \quad (12)$$

$$I_D = \frac{w}{L} \cdot C_i \mu (V_G - V_T) V_D \quad (13)$$

Where, V_T denotes the threshold voltage, C_i is the specific insulator capacitance and W/L is the ration of channel width and length. Thus by using suitable geometry of short channel length L the performance of OFETs can be turned to some degree.

(iv) In organic light-emitting devices (OLEDs) the device operation is governed by injection of charge carriers from contacts. To create balanced charge carrier flow low energetic barriers are created at the metal-organic interface for both contacts to eject equal quantities of holes and electrons. This energetic interface structure plays a very important role for the efficiency of OLEDs [61]. Space charge-limitation of the current is another key approach. Materials with low mobility yield enough current densities for display functions due to the applied high electric field. Photophysical process also affects the efficiency of OLEDs strongly.

Since the photovoltaic effect in organic solids was first observed 1959 in anthracene crystals [62], three main solid state device concepts have been emerged. In the following section a short overview of most successful approaches towards organic solar cells are discussed.

Organic Solar Cells Based on Vacuum Deposited Small Molecules

The concept of this device is based on the thermal evaporation of at least two p and n-conducting materials. The absorption of light in the respective organic materials generates excitons. While these excitons travel to an interface between the n- and p-conducting layers they are splitted into free electrons and holes due to the energetic condition present in p-n junction. Finally the respective carriers are carried towards their electrodes. And this p-n junction can be realized as heterojunctions or bulk heterojunctions.

The small molecule organic solar cells were fabricated using porphyrins and low molecular weight chlorophyll like dye based phthalocyanines [63]. Immense development has been made in the research since 1986 when Tang [64] showed a 1% efficient bilayer heterojunction solar cell based on perylene tetracarboxylic derivative (PTCBI) and copper phthalocyanine (CuPc).

Unfortunately the main advantage and disadvantage of this fabrication process is the process itself. The high cost and complexity of high vacuum technology is a drawback toward commercialization.

Polymer Based Organic Solar Cells

Polymer solar cells have the similar device architecture to those used for small molecule cells. Because of very high molecular weight polymers can't be thermally evaporated so the fabrication differs remarkably. Therefore bulk heterojunction and heterojunction polymer cells are solution processed in contrast to small molecule based organic solar cells. Semiconductor polymers such as the fullerene C60 and P3HT (poly(3-hexulthiophene)) are used to fabricate organic solar cells since 1992 [65]. In contrast to

the small molecule based organic solar cells these materials can be made soluble. And because of that deposition of organics by inkjet printing, screen printing, doctor blading and spray deposition is possible. Additionally, these devices can be fabricated on plastic substrate for flexible devices since these deposition techniques require low temperature. No expensive vacuum technique is required since polymer solar cells can be fabricated under ambient temperature.

Dye-Sensitized Solar Cells

In 1991 Gratzel invented the cell concept of dye-sensitized solar cells. Since then it has attracted wide attention [66]. Dye-sensitized solar cell device concepts are based on a mesoporous nanocrystalline TiO_2 film. A transparent FTO electrode is attached to this film. A monolayer of dye covers the particle in the TiO_2. An organic p-conductor or a liquid electrolyte is used to connect the counter electrode. This p-conductor or liquid electrolyte penetrates into the pores of the TiO_2 network. When excited by light, a dye molecule injects one electron into the TiO_2, which produce a positively charged dye molecule. The charge separation needed for a photovoltaic cell is created by this phenomenon. The counter electrode donates the electrons to a positively charged dye via the electrolyte. This brings back the dye molecules to their original state.

Since dye-sensitized solar cells has potential for low production costs, considerable efforts have been undertaken to enable a commercial up-scaling of this type of organic solar cells.

CHAPTER 3

FABRICATIONS OF ORGANIC SOLAR CELLS

Experimental Methods

In this chapter organic solar cell processing technologies that are used during this work is reviewed. Also the fabrication process of an organic solar cell based on a composite of fullerene derivative [6,6]-phenyl-C61 butyric acid methyl ester (PCBM) and regioregular poly (3-hexylthiophene) (P3HT) with an added interfacial layer of AgOx between the PEDOT:PSS layer and the ITO layer is discussed.

Material Purification

To ensure the device performance and lifetime it is extremely important to purify the organic materials [66]. For example, in crystal the low temperature hole mobility is reduced when anthracene is doped impurity content as low as 10^{-7}g/mol. Though, this level of purity is not comparable to Si or other inorganic semiconductors. There are several chemical purification techniques such as recrystallization, distillation, extraction and absorption, to purify the synthesized materials. Up to 99.9% purity can be achieved through these purification processes [67,68]. This level of purity means that there will be on average one impurity molecule in 1000 molecules. This will possibly modify the optical and electrical properties in an undesirable way. Hence, for optoelectronic applications this level of purity is insufficient.

The source material can further be purified by gradient sublimation [66]. In the process the material is condensed into a quartz tube in vacuum and along the length of the tube a temperature gradient is established. There is a special kind of separation between the compounds due to the temperature gradient [66]. From visual examination one can decide

which product has the highest purity. Usually the pure product has color or textured structure. This procedure can be carried out multiple times to achieve highest possible purity. The condensation temperature and thermal decomposition of the target compound determines the achievable purity.

The Substrate

Patterned ITO coated glass substrates were used to prepare all the devices. First the substrates were cleaned in sequential ultrasonic baths of acetone, methanol, and isopropanol. Prior to the fabrication process of organic devices the ITO coated glass substrate were exposed to UV-ozone for 15 mins. When the substrate was ready AgOx layer was then deposited on top of ITO.

Spin-Coating

For the deposition of photoactive and insulating layers spin-coating technique was used. In this process a small amount of a liquid is dispensed on the substrate. Then it is accelerated to a spin speed typically in the range of 100 rpm to 6000 rpm. Due to the evaporation and flow of the fluid a solid film is formed. Spin speed controls the thickness of the organic layers. The sources are located below the substrate so that dust and flakes do not fall onto the substrate. The source material can be used in powder, granular, and liquid form. And they can be held easily inside the crucible by gravity. Since molecular transport through vacuum in nearly instantaneous, escape rate of molecules from the solid limits the evaporation rate. And the deposition rate is controlled by the source temperature. Typically the deposition rate in the range of 0.1 nm/s to 1 nm/s. The use of substrate and source shutter allows A-level control of the thickness. To monitor the actual deposition rate and film thickness Quartz crystals are used. An unlimited number of

layers can be deposited by thermal vacuum deposition. This is an important advantage compared to spin-coating. A detail explanation of device fabrication is discussed later.

Vacuum Deposition

For depositing low weight organic compounds thermal vacuum deposition is most commonly used [66]. In this process the compound is sublimated from a resistively heated boat or crucible in vacuum (about 10^{-6} Torr to 10^{-10} Torr) [66,69]. The molecular beam is collimated by the elongate shape of the crucible. Usually the mean free path of the evaporated molecules is longer than the chamber. Thus, the molecules are able to travel to the substrate from the source without making any collision with the molecules inside the chamber.

Current –Voltage (IV) Measurement setup

The precise measurement of current and voltage of the fabricated organic solar cells is very crucial. And all the devices on each substrate have to be measured in a decent time. Hence, it is necessary to to measure all cells one after another within the exactly same time span. Doing this will minimized the errors due to the fluctuation of light spectrum emitted by the AM 1.5 solar simulator.

X-Ray Photoelectron Spectroscopy

One of the most important method for mapping out the density of occupied states of a given material is direct X-ray photoelectron spectroscopy (XPS). When a photon is injected into the sample, it excites an electron from an occupied state to unoccupied state. The electron can escape from the solid into the vacuum and can be detected if has energy high enough to ionize. XPS determines the chemical bonding and chemical environment of an element by establishing chemical shifts of specific core levels.

Experimental Details

Because of the low temperature and cost fabrication effective process, organic solar cells (OSCs) offers tremendous promises as an alternative to their counterpart Si based PVs [70-73]. The development of new designs, new materials and interfacial layers facilitate the evolution of OSCs over the past two decades [74,75]. Bulk-heterojunction (BHJ) structures are one of the most promising alternatives to the more expensive silicon solar cells. Effective charge carrier extraction from the active layer to respective electrode is essential for optimal functioning of OSCs. One way to obtain efficient charge extraction is to match the work function of anode and cathode with the highest occupied molecular orbital (HOMO) and lowest unoccupied molecular orbital (LUMO) energies of the active layer [76,77]. The introduction of self-assembled mono-layers of molecules on ITO substrates with appropriate direction and magnitude of dipole moment, improves the performance of organic solar cells [78]. This method decreases the injection barrier between the HOMO level and the ITO and it also effectively changes the work function of ITO. Another way to increase the efficiency is the formation of an interfacial energy step [79,80].

A blend of regioregular poly(3-hexylthiophene) (P3HT) and the fullerence derivative [6,6]-phenyl-C61 butyric acid methyl ester (PCBM) is studied and researched widely to fabricate OSCs [81]. A phase-seperated nanostructure is formed by this blend. The BHJ offers a large interfacial area for efficient excition dissociation [82]. For anode contact a thin poly(3,4-ethylenedioxythiophene):poly(styrenesulfonate) (PEDOT:PSS) layer is used on the top of the anode. Since the work function of PEDOT:PSS matches well with the HOMO of P3HT, holes are extracted effectively from the active layer. There are other

benefits for using PEDOT:PSS. It ensures high electrical conductivity and low temperature solution processability. For these reason is acts as an ideal hole transport material in flexible organic solar cell devices. But its electrical inhomogeneity prevents it to be anefficient electron blocking layer [83]. It might also degrade the device performance due to its acidic and hygroscopic nature. Different metal oxcides like MoOx, VOx, NiOx, and WOx have been used as a substitute to PEDOT:PSS. But metal oxcides form rough interfaces. Device performances is degraded because of the rough interfaces [84-86]. In this work, we added an AgOx interfacial layer in between the ITO and PEDOT:PSS. The AgOx and PEDOT:PSS layers from a composite hole transport layer.

Reagents and Materials

PEDOT:PSS (CleviousPVP AI 4083) was purchased from H.C> Stark Company. The electron donor material regioregular poly (3-hexylthiophene) (P3HT) was purchased from Reike Metals, Inc. [6,6]-phenyl C61 butyric acid methyl ester ($PC_{61}BM$) and 1,2-dichlorobenzene waspurchased from Sigma Aldrich. All these chemicals were used as-received without further purification.

Electrode Modification

Patterned ITO coated glass substrates were used to prepare all the devices. First the substrates were cleaned in sequential ultrasonic baths of acetone, methanol, and isopropanol. Then an ultraviolet ozone (UVO) treatment was applied on the substrate for 15 mins. When the substrate was ready AgOx layer was then deposited on top of ITO. At first, 1 nm thick Ag metal was deposited by thermal evaporation at a pressure of $\sim 10^{-7}$ Torr. Then it was placed for an UVO treatment for 1 min. This led to the formation of AgOx. The formation of AgOx layer was confirmed by X-ray photoelectron spectroscopy

(XPX) analysis. With the help of an Ocean Optics double channel Spectrometer (model DS200) the optical transmittance of bare ITO and AgOx modified ITO electrodes were measured in a wavelength range of 300-800 nm. The oxidation state of Ag in the modified ITO electrode was determined by XPS using a VG-220IXL spectrometer with

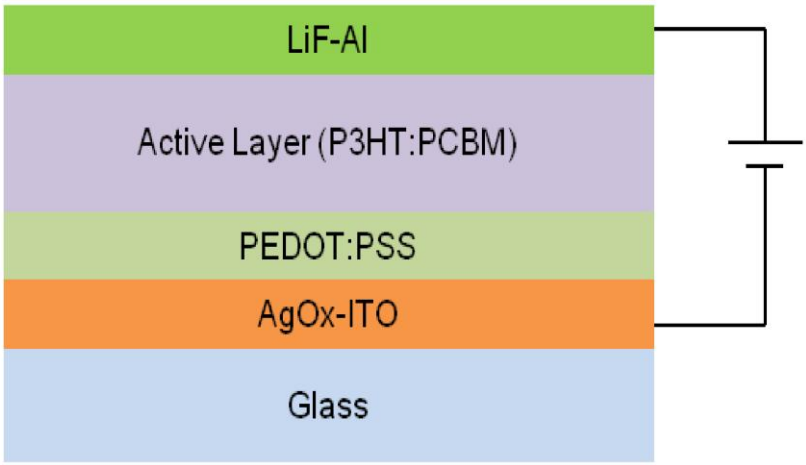

Fig. 6. Device structure of AgOx based OSC.

monochromatic Al *Kα* radiation (1486.6 eV, line width¼0.8 eV). The pressure in the analyzing chamber was kept at a level of 10_9 Torr while recording the spectrum. The spectrometer had an energy resolution of 0.4 eV. All the binding energies were corrected with reference to C (1-s) at 284.6 eV.

Device Fabrication

Electron acceptor material $PC_{61}BM$ and donor material P3HT were weighted (1:1 w/w). After that they were dissolved in 1,2-dichlorobenzene (DCB) in a nitrogen-filled glove box. The solution was stirred for a minimum of 12 hours at room temperature. Then on a freshly prepared electrode PEDOT:PSS solution was spin-coated at 5000 rpm for 60s.

After that it was left on a hot plate at 150^0C for 15 mins. After annealing, the photoactive layers were spin-coated at 600 rpm for 1 min from the P3HT:PC_{61}BM blends. The substrate was then heat annealed for 30 mins at 120^0C inside the nitrogen filled glove box. A layer thickness of 250nm was achieved from this.

Finally, in vacuum 0.7 nm of LiF was deposited by thermal deposition followed by 80nm thick Al cathode. An active area of 0.2 cm^2 was defined by using shadow mask during thermal evaporation. Both of the devices (control and AgOx modified) were tested in a solar simulator. Fig. 6 shows the device structure of the AgOx interfacial layer based OSC.

Device Testing

A xenon-lamp solar simulator (Spectra Physics, Oriel Instrument, USA) was used to generate AM 1.5 global solar irradiation (100 mW/cm^2). Under this simulated solar irradiation current density-voltage (J-V) measurements were performed. Using a standard Si photodiode reference cell the light source was calibrated. The external quantum efficiency (EQE) was measured as a function of wavelength from the photocurrent generated in the device from an incident monochromatic light source.

CHAPTER 4

EQUIVALENT CIRCUIT MODEL FRO ORGANIC SOLAR CELLS

Basic Component of ECD

The electric systems of organic solar cell are very complex. In order to understand the electric behavior and observe how the parameters changes with any kind of treatment applied to the device, it is modeled using electrical components such as voltage or current sources, diodes and resistors. It provides a scientific and realistic physical explanation for the OPV behavior. Followings are the most general components in the Equivalent Circuit Diagram (ECD) of an organic solar cell device.

The specific physical processes in organic semiconductor might vary from that of the inorganic semiconductors therefore lead to other parameters. But their principle loss mechanisms are the same. So the same equivalent circuit can be used for both of them. Followings are the most common components in ECD.

Current Source

The current source represents the generation of current I_L upon illumination. It is defined as the number of electron-hole pairs before any recombination can take place.

Shunt Resistance

The shunt resistance is formed near the D/A interface due to the recombination of charge carriers. It has at least one order of higher magnitude than the series resistance R_s. The shunt resistance also includes the recombination that takes place near the electrode (away from dissociation site) or an extra resistance in shunt has to be added. Usually R_{sh} is measured by taking the inverse slope at around 0 V. Because around 0V the diode does

not conduct and the total current is determined by $R_{sh} + R_s$ where R_{sh} is much larger than R_s.

$$R_{SH} \approx \left(\frac{I}{V}\right)^{-1} \tag{14}$$

Series Resistance

The conductivity of the specific charge carrier is represented by series resistance R_s. The value of R_s increases with thicker transport layers. R_s is also affected by the space charges and traps because it affects the mobility or the charge carriers. At higher external positive voltage the diode becomes conductive and R_s dominates the shape of the IV curve. At that point where the IV curve becomes linear the value of R_s can be measured by taking the inverse slope.

$$R_S \approx \left(\frac{I}{V}\right)^{-1} \tag{15}$$

Ideal Diode

The built in field due to the difference between the donor HOMO and acceptor LUMO level creates an asymmetry of conductivity which is represented by a voltage dependent resistor or the ideal diode D. In single layer cells it may also represents the nature of the semiconductor electrode blocking contact. The nonlinear shape of the IV curves is due to the diode. If $R_{sh} \cong \infty\Omega$ and $R_s = 0\Omega$, the IV characteristic of the entire cell will be equal to the IV characteristic of the diode.

Solar Cell Voltage

Depending on the load resistance a voltage between 0 and V_{oc} can be generated by the cell. To obtain the IV curve beyond this range an external voltage source is required. It is to be noted that the actual photon to current conversion efficiency of the cell cannot be

increased by the external voltage source. The purpose of this external voltage source is to act as a current amplifier to provide current for $V > V_{oc}$ or $V < 0V$.

These components are sufficient to explain most efficient effects in solar cells of all types. However the most comprehensive ECD for organic devices might comprise the following parameters.

Capacitor

A capacitor C is considered to represent the charging/discharging and other time dependent effect. Usually the area of the cell is larger than the difference between the electrodes so this effect can be significant.

$$C = \in (\frac{A}{d})^{-1} \tag{16}$$

Second Diode

Holes at the ITO electrode from an extra blocking contact that can affect the IV cure in the third quadrant. This can also lead the FF value less than 0.25. If a sufficiently high voltage is applied the electrons at ITO and the holes at the metal allow charge injection.

Extra Shunt Resistor

The shorts due to significant conductivity of the bulk material and the pinholes are represented by an extra shunt resistor. The recombination losses near the electrodes may also be accounted by the resistor. If R_s is considerably smaller than both of the shunt resistance, the effect of R_{sh2} can be considered with R_{sh}.

Ideal Solar Cell

Solar cells are semiconductor with a p-n junction fabricated in a thin wafer or layer of semiconductors. A photo current is generated when it is exposed to light. The photo current is proportional to the intensity of the solar radiation. In the dark, the I-V curve of the solar cell has exponential characteristics like a diode [84].

To obtainthe maximum output power from PV power plant the understanding and modeling of PV cell is necessary [85]. A current source in parallel with a single-diode is the ideal equivalent circuit of a solar cell. PV solar cells typically can be represented by an equivalent circuit consisting of a single diode as shown in Fig. 7 The resistor and current values depend on the illuminated area. But the dark current depends on the actual device area.

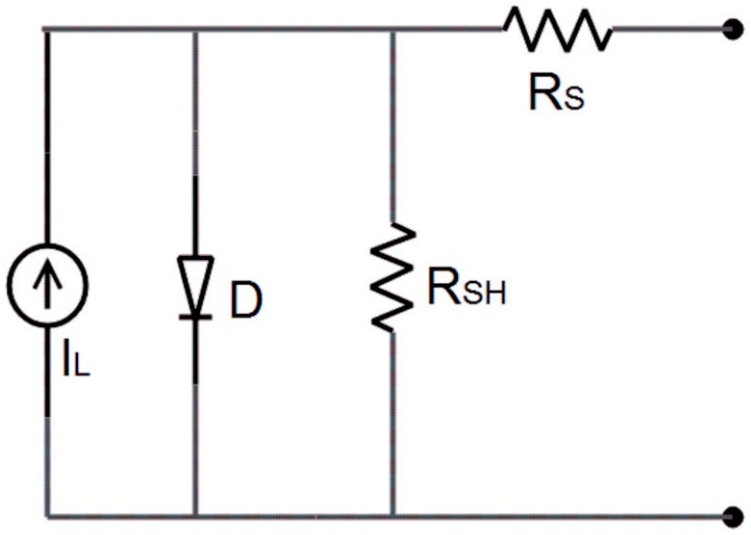

Fig. 7. Single diode model equivalent circuit.

Assuming that, for voltage dependence of the current the Shockley diode equation can be used and I_D is the current through the ideal diode D then applying Kirchoff's current and voltage laws in currents nodes and voltage loops we can formulate the following equation:

$$(I_L - I_D - I)R_{SH} = V + IR_S \tag{17}$$

which, can be written as:

$$I(\frac{R_S}{R_{SH}} + 1) = I_L - I_D - \frac{V}{R_{SH}} \tag{18}$$

by Shockley diode equation we can show the voltage dependence of the current through the ideal diode D

$$I_D = I_0[\exp(\frac{V + IR_S}{nkT / q}) - 1] \tag{19}$$

in equation [18] if we replace the value of I_D from equation [19] we get:

$$I = (I_L - \frac{V}{R_{SH}}).\frac{R_{SH}}{R_{SH} + R_S} - I_0.[\exp(\frac{V + IR_S}{nkT/q}) - 1].\frac{R_{SH}}{R_{SH} + R_S} \tag{20}$$

This equation is used to describe to I-V curve characteristics. This equation needs numerical method to find the solutions. Organic solar cells often suffer from high series resistors and small shunt resistance. As such, the I-V curve of organic solar cell is different than the inorganic solar cells.

If we consider an ideal solar cell with only an ideal diode D in the dark such that the series resistance $R_S = 0$ and the shunt resistance $R_{SH} = \infty$. From equation 19 we obtain

$$I_D = I_0[\exp(\frac{V}{nkT/q}) - 1] \tag{22}$$

The current through the diode represents the current through the solar cell. It is this current that is given by the Shockley diode current equation - I increase exponentially with the voltage V. When the cell is illuminated under the light it generates a photo current I_L. This current is simply added to the normal I-V characteristics of the diode D. The relation is given by:

$$I_D = I_0[\exp(\frac{V}{nkT/q}) - 1] - I_L \quad (23)$$

The addition of the current I_L results in a region of fourth quadrant in the I-V curve. Electrical current can voltage can be extracted from the fourth quadrant. Maximum voltage results when I_L manages to cancel the dark current. For constant value of I_L, the dark current decreases with increasing value of V_{OC}. And the current I_0 determines the height of the curve. The voltage at which the current value is zero (I - 0) is called the open circuit voltage (V_{OC}). So by putting I = 0 in equation 21 we get the open circuit voltage V_{OC}:

$$V_{OC} = \frac{nkT}{q}.\ln(\frac{I_L}{I_0} + 1) \quad (24)$$

Effect of Shunt Resistance

By setting the output current to zero (I=0) in Eqn. 22 - a formula for V_{OC} shows the influence of R_{SH} can be determined [28].

$$V_{OC} = \frac{nkT}{q}\ln(\frac{I_L - V_{OC}/R_{SH}}{I_0} + 1) \quad (25)$$

Equation 24 relates the maximum output voltage with the photo generated, reverse saturation current, and the shunt resistance. V_{OC} is related to the ration of I_L/I_0. As, I_L is decreased by R_{SH} there is no current flowing through R_S. This means R_S cannot create a

voltage drop loss. So, both the ideal diode D and the shunt resistor determine V_{OC}. For example, suppose the cell is in the dark and R_{SH} is small. Now if we apply an external voltage across the cell electrode then the voltage drop across R_{SH} and the Diode D will be equal. It is the current through the diode that will determine the shape of the I-V characteristics [86]. The sum of the current through diode D and the shunt resistance R_{SH} gives the current through the electrode.

Upon illumination a current I_L will be generated and it will pass through the diode D and R_{SH}. Since *n* is out of the logarithm function is has a greater influence on V_{OC} than R_{SH} and I_0. R_{SH} can have serious effect on V_{OC} and can decrease it sufficiently.

Effect of Series Resistance

Organic solar cells often have larger series resistance. That means current measured in the short circuit has to go through a large resistor. This will seriously limit the output current if R_{SH} is also small. R_S can also reduce the open circuit voltage if it reaches the value to large shunt resistance. But recombinations that take place near the electrode (represented by R_{SH}) in the device are more effective in decreasing V_{OC} than the recombination in the middle of the device which is represented by R_S.

The Two Diode Model

The two-diode model can be described from the lumped parameters of Fig. 8. Using the Shockley diode equations we obtain:

$$I = (I_L - \frac{V}{R_{SH}})\frac{R_{SH}}{R_{SH}+R_S} - I_{01}[\exp(\frac{V+IR_S}{nkT/q}) - 1] \cdot \frac{R_{SH}}{R_{SH}+R_S} - I_{02}[\exp(\frac{V+IR_S}{nkT/q}) - 1]\frac{R_{SH}}{R_{SH}+R_S} \quad (26)$$

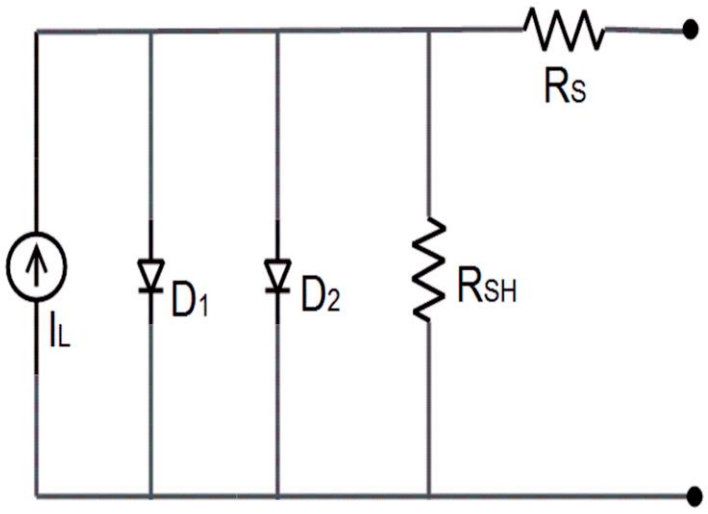

Fig. 8. Two diode model equivalent circuit

Setting I = 0 we get the equation for Voc which is

$$V_{OC} = \frac{nkT}{q} \ln\left(\frac{I_L - V_{OC}/R_{SH}}{I_{01} - I_{02}} + 1\right) \tag{26}$$

Lower mobility and smaller charge carrier concentration lead to considerably smaller currents in most organic solar cells. In fact, both the dark and light currents are about 1000 times smaller; hence, the light current in these devices is about as large as the dark current in silicon devices. The dark current is still about 900 times smaller and according to (26) a similar V_{OC} is expected.

CHAPTER 5

DATA ANALYSIS AND RESULTS

Experimental Results

To analyze the different oxidation states of the AgOx thin film XPS analysis is utilized on the sample consisting of UVO-treated 1nm Ag on ITO. The corresponding binding energy for AgOx was found to be 368.2 eV and 367.8 eV and. These are consistent with those of Ag_2O and AgO respectively. After ozonization the Ag^{2+} to Ag^{+} ratio was 72:28 which indicate that Ag^{2+} is the dominant silver oxidation state in the thin film. In the AgOx films on ITO the information about the chemical state of oxygen was found by deconvolution of the O 1s spectrum. The AgOx is a p-type semiconductor. And depending on the processing condition its work function varies from 4.7 to 5.2 eV. [87].

The added interfacial layer plays an important role for charge carrier transport and collection. Defects are formed if the surface is rough near the electrode surface which can decrease the power conversion efficiency [29]. The rms roughness of bare ITO was 0.5nm. But after adding AgOx layer the rms roughness increased to 4.2nm. So, the surface morphology was increased by adding the AgOx interfacial layer. Due to evaporation there were some Ag islands, so the ITO wasn't totally covered by the AgOx layer.

Many previous investigation showed that P3HT:PC_{60}BM blend of 1:1 weight ratio has an absorption band of 400-600nm. And for annealed films the maximum absorption wavelengths are ~ 510nm [88,89]. The optical transmittance of bare ITO and AgOx/ITO layer is shown in Fig. 9 over the range of 400-800nm. Over this range the average range of transmittance of ITO was 77% but with the AgOx layer the transmittance slightly

reduced down to 74%. This reduced the number of absorbed photons passing through the anode and correspondingly decreased photocurrent generation. Figure 10(a) shows the current density-voltage characteristic curve for the device in the dark. Form the characteristics curve it is visible that the current density was significantly increased in the added AgOx layered device than the bare ITO device. Under AM 1.5 illumination with an intensity of 100 mW/cm^2 the J-V characterstics curve of the device is shown in figure 10(b). Since the active layer fabrication condition and the cathode layer deposition remain constant there is no change in the open circuit voltage condition.

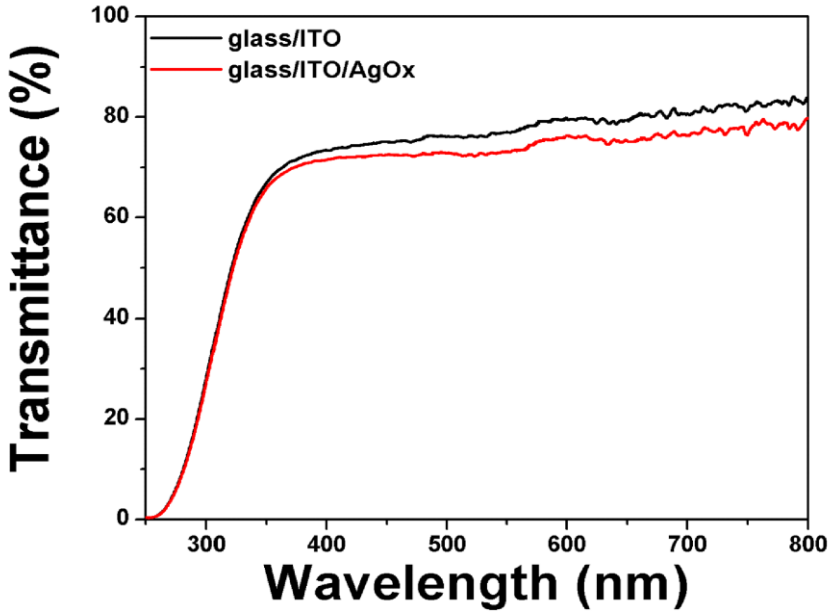

Fig. 9. Optical Transmittance of bare and AgOx/ITO films. [90]

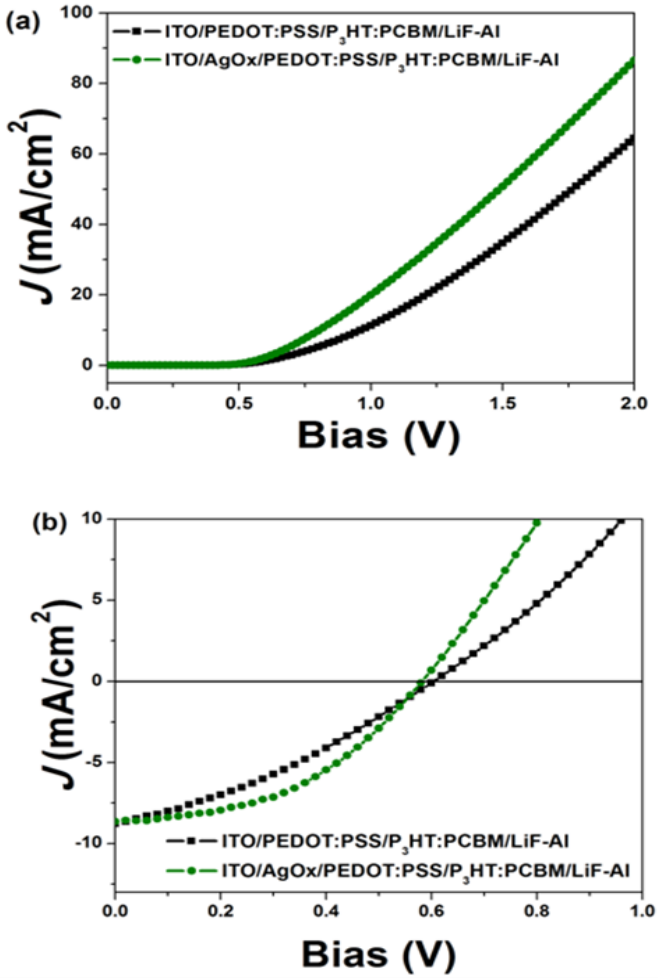

Fig. 10. Current-density (J-V) characteristics of the bulk-heterojunction solar cell with bare ITO and AgOx/ITO anode layer (a) in dark and (b) under illumination (AM 1.5, 100 mW/cm2) [90].

The device with ITO/PEDOT:PSS anode showed a power conversion efficiency of 1.74%. The short circuit current density (J_{SC}) and the open circuit voltage of the device were respectively, 8.76 mA/cm^2 and 0.60 V. For the added AgOx layer device both values were slightly reduced (J_{SC} =8.64 mA/cm^2 and V_{OC}= 0.58V).

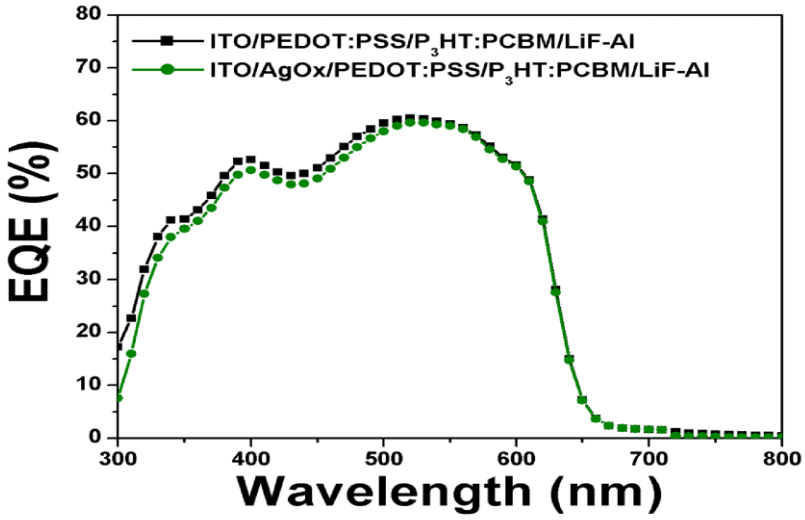

Fig. 11. EQE measurement of the P3HT:PCBM devices using bare ITO and AgOx/ITO anodes [90].

But the power conversion efficiency (PCE) and the fill factor (FF) were increased. The fill factor was increased by 36% with the added interfacial AgOx layer. The EQE results of the device with and without AgOx layer is shown in Fig. 11. Both devices showed EQE values over 50% with efficient photo conversion efficiency within the range between 400 and 600nm. The experimental values of the device parameters of the organic solar cells are given in table 2 [90].

Table 2:

Device Parameters of the Fabricated Organic Solar Cells

Anode	J_{SC} (mA/cm^2)	V_{OC} (V)	FF(%)	PCE(%)	R_S (Ωcm^2)	R_{SH} (Ωcm^2)
ITO	8.76	0.60	33	1.74	28	150
AgOx/ITO	8.64	0.58	45	2.25	18	587

Under illumination the OSC may be modeled by an equivalent circuit (ECD). The current equation for single diode model and two diode model is given by equation (20) and (26). But to understand the characteristic of our device a modified ECD is proposed. This modified ECD was able to explain the device characteristic clearly.

Proposed Model:

According to (26) both the ideal diode D and R_{SH} are now the components that determine V_{OC}. This assumes that R_{SH} is not very high and the device is in the dark and by applying a positive voltage across the cell electrodes a voltage drop can be created across R_{SH} which equal to the voltage V_D across the ideal diode D. The current that can pass through the diode D at V_D is determined by its I-V characteristic. The sum of the currents through D and R_{SH} yields the current through the electrodes of the solar cell for a given applied voltage. Upon illumination, the current source generates the current I_L some of which passes through the diode where a voltage drop is generated that is big enough to allow the rest of I_L to go through R_{SH} if the electrodes are open. The same voltage can be measured with a voltmeter with high internal resistor across the device electrodes and is then termed open circuit voltage Voc.

Fig. 12 shows that the I-V characteristics changes if the shunt resistance varies between 100 ohm and 3000 Ohm assuming the shown values for R_S, I_L, and I_O. If R_{SH}> 1500 Ohm the shape (FF,V_{OC}) of the IV curves remains virtually unchanged and the current shows no significant field dependence for negative bias.

However, clearly smaller R_{SH} values have detrimental effects on the IV curve. The slope (field dependence) in the third quadrant increases considerably, V_{OC} approaches zero and

the FF reaches its theoretical minimum of 0.25 very quickly. However, the short circuit current is not affected since the current through the shunt can be neglected if $R_S << R_{SH}$.

Fig 13 shows the I-V characteristics with increasing series resistance, assuming the same parameters as above. While the slope in the third quadrant remains unchanged the slope in the first quadrant starts to decrease considerably when R_S reaches the same order of magnitude as R_{SH}. The effect of the large R_S even extends into the third quadrant thereby decreasing FF to its minimum.

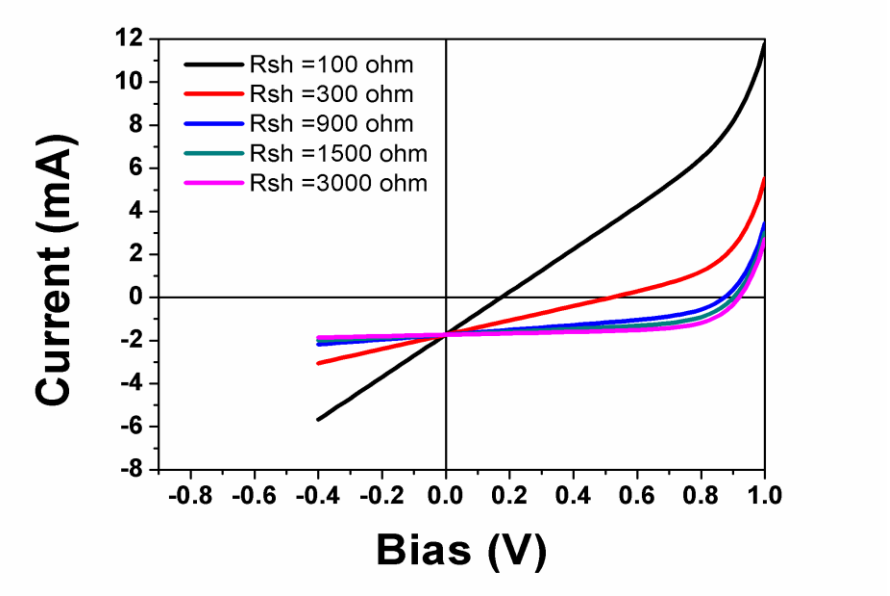

Fig. 12. Effect of R_{SH} with hypothetical value of R_S = 1Ohm (device area 0.2 cm^2), under 100mW/cm^2 illumination intensity.

Moreover, if the two resistors have similar values, the I-V curve is dominated by their Ohmic characteristics (the inverse slope in the 1 quadrant is equal to R_S) and the ideality factor or voltage dependence of D may then have little influence. Note that in contrast to the effect of R_{SH} the short circuit current can decrease but the open circuit voltage cannot be affected at all- since there is no current through R_S at V_{OC}.

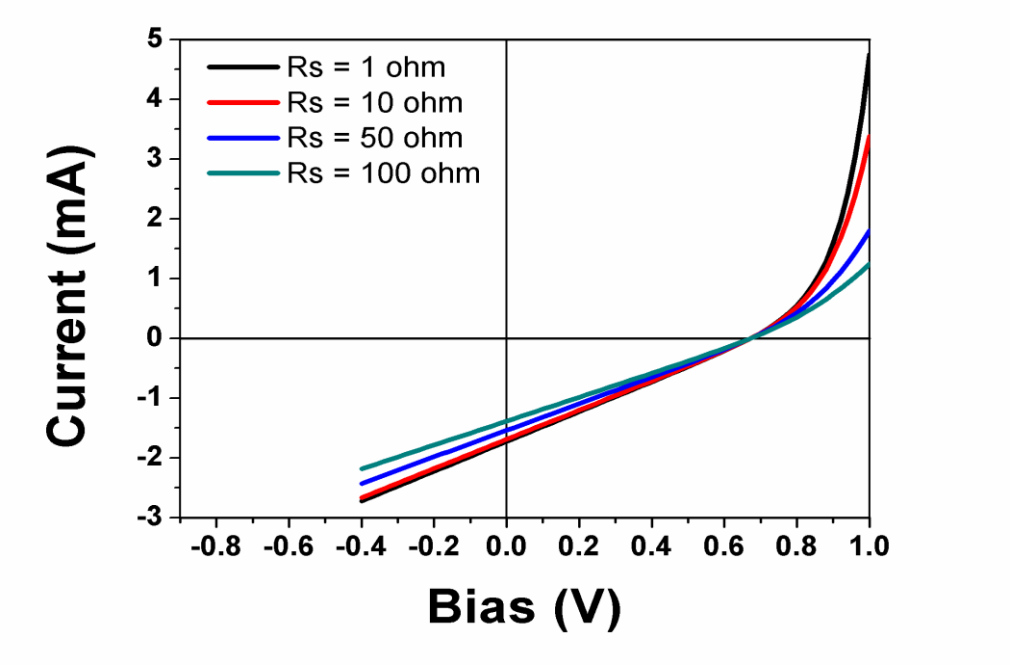

Fig. 13. Effect of R_S with hypothetical value of R_{SH} = 400 Ohm (device area 0.2 cm^2), under 100mW/cm^2 illumination intensity.

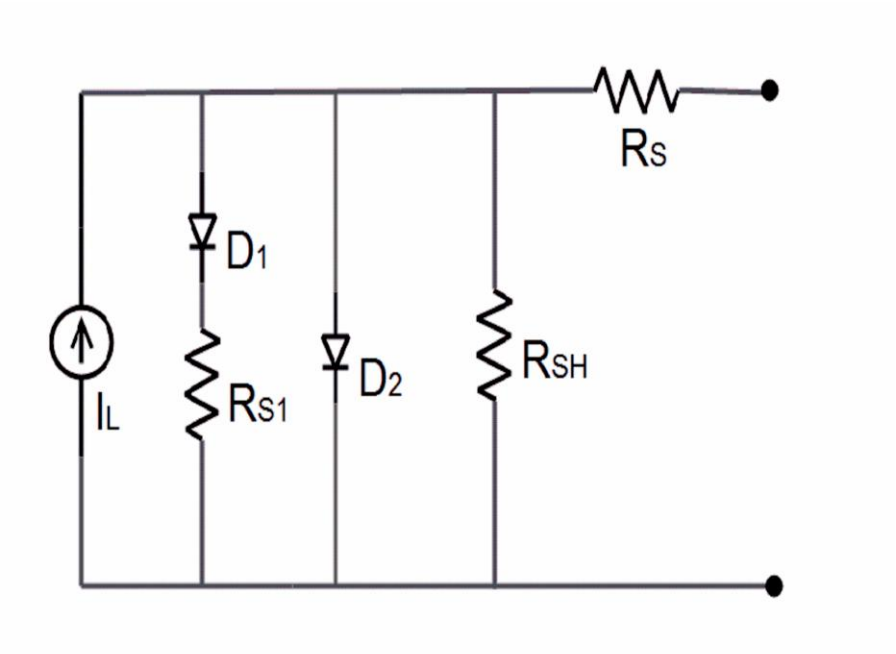

Fig. 14. Proposed two diode model equivalent circuit.

Once all the parameters for the equivalent circuit are determined, using the raw data we have constructed simulated I-V plot in order to develop a model that best describe this particular OSC. Considering the effect of R_{SH} and R_S as discussed above, a resistor R_{S1} in series with one diode is added. R_{S1} accounts for the recombination of the carriers. Fig. 14 shows the proposed model. The ideality factor *n* for both of the diodes was assumed equal with an approximation corresponding to the Shockley-Read-Hall recombination current density in the space-charge region [32]. The current equation for the proposed two diode model is given by equation (7).

$$I = (I_L - \frac{V}{R_{SH}})\frac{R_{SH}}{R_{SH}+R_S} - I_{01}[\exp(\frac{V+IR_S+IR_{S1}}{nkT/q})-1]\cdot\frac{R_{SH}}{R_{SH}+R_S} - I_{02}[\exp(\frac{V+IR_S}{nkT/q})-1]\frac{R_{SH}}{R_{SH}+R_S} \quad (7)$$

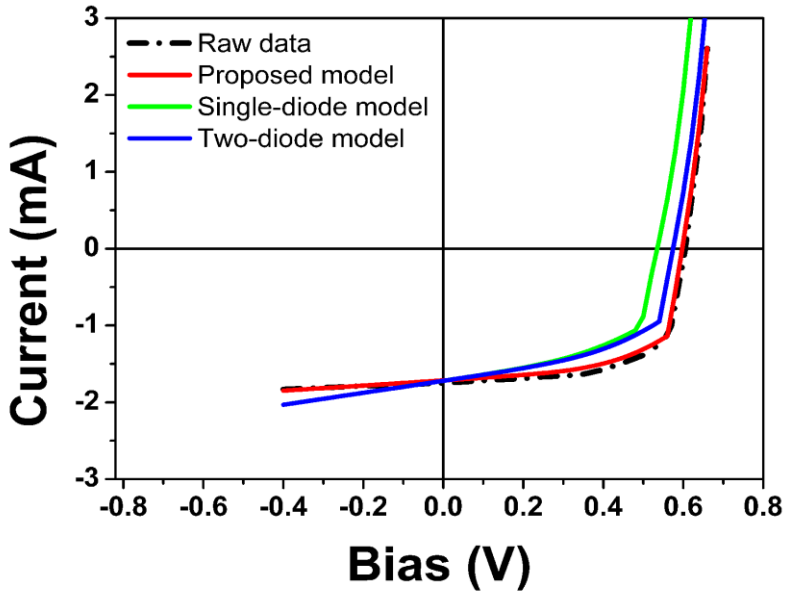

Fig. 15. Simulated and experimental curves of I-V characteristics for the organic solar cell under 100mW/cm^2 illumination (device area 0.2 cm^2).

Fig. 15 shows the I-V plots for experimental data and simulated plots for the proposed model, single and two diode models under 100mW/cm^2 illumination intensity. It is observed that the I-V characteristics generated from our proposed model fits well with the experimental result. The average percentage variation is 2.38%. Using a AgOx interfacial layer between PEDOT:PSS and ITO increases the power conversion efficiency by 28%.

REFERENCES

[1] Hassan, H.Z., A.A. Mohamad, and H.A. Al-Ansary (2012). Development of a continuously operating solar-driven adsorption cooling system: Thermodynamic analysis and parametric study. Applied Thermal Engineering, 48(0): p. 332-341.

[2] . Hassan, H.Z. and A.A. Mohamad, A review on solar-powered closed physisorption cooling systems. Renewable and Sustainable Energy Reviews, 2012. 16(5): p. 2516-2538.

[3] Afshar, O., et al. (2012) A review of thermodynamics and heat transfer in solar refrigeration system. Renewable and Sustainable Energy Reviews 16(8): p. 5639-5648.

[4] Wang, D.C., et al. (2010) A review on adsorption refrigeration technology and adsorption deterioration in physical adsorption systems. Renewable and Sustainable Energy Reviews 14(1): p. 344-353.

[5] Hassan, H.Z. and A.A. Mohamad (2012). A review on solar cold production through absorption technology. Renewable and Sustainable Energy Reviews 16(7): p. 5331-5348.

[6] Balaras, C.A. (2007). et al., Solar air conditioning in Europe—an overview. Renewable and Sustainable Energy Reviews 11(2): p. 299-314.

[7] Li, Z.F. and K. Sumathy (2000).Technology development in the solar absorption air-conditioning systems. Renewable and Sustainable Energy Reviews 4(3): p. 267-293.

[8] Kalkan, N., E.A. Young, and A. Celiktas (2012). Solar thermal air conditioning technology reducing the footprint of solar thermal air conditioning. Renewable and Sustainable Energy Reviews 16(8): p. 6352-6383.

[9] Choudhury, B., P.K. Chatterjee, and J.P. Sarkar (2010). Review paper on solar-powered air-conditioning through adsorption route. Renewable and Sustainable Energy Reviews 14(8): p. 2189-2195.

[10] Turanjanin, V. (2009). et al., Fossil fuels substitution by the solar energy utilization for the hot water production in the heating plant “Cerak” in Belgrade. International Journal of Hydrogen Energy 34(16): p. 7075-7080.

[11] Phuangpornpitak, N. and S. Kumar, PV hybrid systems for rural electrification in Thailand. Renewable and Sustainable Energy Reviews, 2007. 11(7): p. 1530-1543. Nayar, C.V. (1993). et al., Novel wind/diesel/battery hybrid energy system. Solar Energy,. 51(1): p. 65-78.

[12] Exposed: U.N. Intergovernmental Panel On Climate Change IPCC (2015.). Retrieved July 8.

[13] Tsuzuki, T., Shirota, Y., Rostalski, J., & Meissner, D. (n.d.). The effect of fullerene doping on photoelectric conversion using titanyl phthalocyanine and a perylene pigment. Solar Energy Materials and Solar Cells, 1-8.

[14] Green, M., Emery, K., Bücher, K., King, D., & Igari, S. (n.d.). Solar cell efficiency tables (version 12). Progress in Photovoltaics: Research and Applications Prog. Photovolt: Res. Appl., 265-270.

[15] Shockley, W., & Queisser, H. (n.d.). Detailed Balance Limit Of Efficiency Of P-n Junction Solar Cells. Journal of Applied Physics, 510-510.

[16] H. J. Lewerenz and H. Jungblut (1995). ”Photovoltaic -Grundlagen und Anwendungen” Springer, Berlin, Heidelberg, New York.

[17] B. O’Regan and M. Graetzel (1991), ”A low cost, high efficiency solar cell based on dye-sensitized colloidal TiO2 films.” Nature 353, 737.

[18] S. Barth and H. Baessler (1997). ”Intrinsinc photoconduction in PPV-Type conjugated polymers.” Phys.Rev.Lett. 79, 4445-4448.

[19] P. G. d. Costa and E. M. Conwell (1993). ”Excitons and the band gap in PPV.” Am.Phys.Soc.-Rap.Comm.48, 1993-1997.

[20] R. N. Marks, J. J. M. Halls, D. D. C. Bradley, R. H. Friend and A. B. Holmes (1994). ”The photovoltaic response in PPV thin film devices.” J. Phys.: Cond. Mat. 6, 1379-1394

[21] J. J. M. Halls, K. Pichler, R. H. Friend, S. C. Moratti and A. B. Holmes (1996) ”Exciton diffusion and dissociation in a PPV/C60 heterojunction photovoltaic cell” Appl.Phys.Lett. 68, 3120-3122.

[22] J. J. M. Halls and R. H. Friend (1996). ”The photovoltaic effect in a PPV/perylene heterojunction.” Synth.Met. 85, 1307-1308

[23] A. K. Ghosh and T. Feng (1978).”Merocyanine organic solar cells. ” J.Appl.Phys. 49, 5982-5989.

[24] V. Choong, Y. Park, Y. Gao, T. Wehrmeister, K. Muellen, B. R. Hsieh and C. W. Tang (1996).”Dramatic PL quenching of PPV oligomer thin films upon submonolayer Ca deposition.” Appl.Phys.Lett. 69, 1492-1494.

[25] A.C. Arias, M. Granstrom, K. Petritsch and R.H.Friend. (1999) ”Organic photodiodes using polymeric anodes” Synth. Met. 102, 953-954.

[26] K. C. Kao and W. Hwang (1981). ”Electrical Transports in Solids - with Particular Reference to Organic Semiconductors” Pergamon Press, Oxford.

[27] R. Farchioni, G. Grosso (eds.) (2001). Organic Electronic Materials. Springer, Berlin.

[28] H. Ago, K. Petritsch, M.S.P. Shaffer, A.H.Windle and R.H. Friend (1999) ”Composites of carbon nanotubes and conjugated polymers for photovoltaic devices” Adv.Mat. 11, 1281-1285.

[4] M. R. Andersson, D. Selse, M. Berggren, H. Jaervinen, T. Hjertberg, O. Inganaes, O. Wennerstroem and J. E. Oesterholm (1994). ”Regioselective polymerization of 3- (4-octylphenyl)thiophene with FeCl3.” Macromolecules 27, 6503-6506.

[30] Fesser, Bishop and Campbell (1983). ”Optical absorption from polarons in a model of polyacetylene” Phys.Rev.B 27 4804-4825.

[31] M.A. Green (1995). Silicon Solar Cells. Advanced Principles and Practice. University of New South Wales, Sydney.

[32] J.P. Wolfe and A. Mysyrowicz (1984) ”Excitonic Matter”Scientific American 250 No.3, 70.

[33] M. Chandross, S. Mazumdar, S. Jeglinski, X. Wei. Z.V. Vardeny, E.W. Kwock and T.M. Miller (1994).J.Phys.:Condens.Matter 6, 1379-1394.

[34] M. Pope and C.E Swenberg (1982) Electronic Processes in Organic Crystals, Clarendon Press, Oxford.

[35] Halls, J.J. and R.H. Friend, Organic Photovoltaic devices, in Clean electricity from photovoltaics, M.D. Archer and R. Hill, Editors. 2001, Imperial College Press: London.

[36] 15. Kepler, R. G. (1960). Phys. Rev. 119, 1226.

[37] .Scher, H.; Montroll, E. W (1975).Phys. Rev. B 12, 2455.

[38] Fink, R.; Heischkel, Y.; Thelakkat, M.; Schmidt, H. W.; Jonda, C.; Hüppauff, M. Chem. Mater. 10, 3620.

[39] Kallmann, H.; Pope, M (1960). J. Chem. Phys. 32, 300.

[40] Pope, M.; Swenberg, C. E (1999). “Electronic Processes in Organic Crystals and Polymers, 2nd ed.” (Oxford University Press, New York.

[41] Malliaris, G.; Friend, R (2005). Physics Today 58, 53.

[42] Shen, Y.; Diest, K.; Wong, M. H.; Hsieh, B. R.; Dunlap, D. H.; Malliaras, G. G. (2003) Phys. Rev. B 68, 081204(R).

[43] McQuarrie, D. A (1983). "Quantum Chemistry" (University Science Books, Sausalito.

[44] Tsutsui, T.; Fujita, K (2002). Adv. Mater. 14, 949. b) Dodabalapur, A (2006). Materials Today 9, 24.

[45] Klinger, M. I.; Sykes, J. B (1979). "Problems of Linear Electron (Polaron) Transport Theory in Semiconductors, 1st ed." (Pergamon Press, New York. Holstein, T (1959). Ann. Phys. 8, 325. Holstein, T (1959). Ann. Phys. 8, 343. Schein, L. B.; Mack, (1988). J. X. Chem. Phys. Lett. 149, 109.

[46] Mozer, A. J.; Denk, P.; Scharber, M. C.; Neugebauer, H.; Sariciftci, N. S. J. Phys. Chem. B 108, 5235 (2004). Pai, D. M. J. Chem. Phys. 1970, 52, 2285.

[47] Gill, W. D (1972). J. Appl. Phys. 43, 5033.

[48] Bässler, H (1993). Phys. Status Solidi B 175, 15.

[49] Borsenberger, P. M.; Weiss, D. S. (1993) "Organic Photoreceptors for Imaging Systems" (Marcel Dekker, New York.

[50] C.W Tang and A.C. Albrecht (1975). J Chem. Phys 62, 2139.

[51] C. Brabec, A. Cravion, D. Meissner, N. Sariciftci, T. Frommherz, M. Rispens, L. Sanchez, and J. C. Hummelen. (2001). Adv. Funct. Mater. 11, 374

[52] B. Rand, D. Burk, and S. Forrest (2007). Phys. Rev. B 75, 115327.

[53] A. Gadisa, M. Svensson, M. Andersson, and O. Inganas (2004). Appl. Phys. Lett. 84, 1609.

[54] M. Schw¨orer and H.C.Wolf (2005). Organische Molekulare Festk¨orper. Wiley-VCH,

[55] N. S. Sariciftci, L. Smilowitz, A. J. Heeger, and F. Wudl (1992). Science 258, 1474

[56] C. J. Brabec, V. Dyakonov, J. Parisi, and N. S. Sariciftci (eds.) (2003). Organic Photovoltaics. Springer, Berlin.

[57] M. Pfeiffer, K. Leo, X. Zhou, J. S. Huang, M. Hofmann, A. Werner, and J. Blochwitz-Nimoth (2003). Org. Electron. 4, 89.

[58] M. Gross, D. C. M¨uller, H.-G. Nothofer, U. Scherf, D. Neher, C. Br¨auchle, and K. Meerholz (2000). Nature 405, 661.

[59] Pope, M.; Swenberg, C. E (1999). "Electronic Processes in Organic Crystals and Polymers, 2nd ed." (Oxford University Press, New York.

[60] Malliaris, G.; Friend (2005). Physics Today 58, 53.

[61] W. R. Salaneck, K. Seki, A. Kahn, J.-J. Pireaux (2002). Conjugated Polymer and Molecular Interfaces.

[62] H. Kallmann and M. Pope (1959). J. Chem. Phys 30, 585.

[63] C.W Tang and A.C. Albrecht (1975). J. Chem. Phys 62, 2139.

[64] C.W. Tang and S.A. VanSlyke (1987). Appl. Phys. Lett. 51, 913.

[65] D. Chirvase, Z. Chiguvare, M. Knipper, J. Parisi, V. Dyakonov, J.C. Hummelen (2003). J. Appl. Phys. 93, 3376.

[66] B. O'Regan and M. Gr¨atzel (1991). Nature 353, 6346.

[67] S.R. Forrest (1997). Chem. Rev. 97, 1793.

[68] K.H. Probst and N. Karl (1975). Phys. Stat. Sol. A 27, 499.

[69] R.J. Doome, A. Fonseca, H.Richter, J.B. Nagy, P.A. Thiry, and A.A. Lucas (1997). J. Phys. Chem. Sol. 58, 1839.

[70] K.C. Khemani, M.Prato, and F. Wudl (1992). J. Org. Chem. 57, 3254.

[71] D.E Bornside, C.W. Macosko, and L.E. Scriven (1987). J. Imaging Technol. 13, 122.

[72] D. Meyerhof (1987). J. Appl. Phys. 49, 3993.

[73] M. Knudsen (1909). Ann. Phys 28, 75.

[74] D. Cahen and A. Kahn (2003). Adv. Mat. 15(4), 271.

[75] C. J. Brabec, N. S. Sariciftci, and J. C. Hummelen (2001). Adv. Funct. Mater. 11, 15–26

[76] F. C. Krebs (2009). Sol. Energy Mater. Sol. Cells 93, 394–412.

[77] H. Y. Chen, J. Hou, S. Zhang, Y. Liang, G. Yang, Y. Yang, L. Yu, Y. Wu, and G. Li (2009). Nat. Photonics 3, 649–653.

[78] J. Y. Kim, K. Lee, N. E. Coates, D. Moses, T.-Q. Nguyen, M. Dante, and A. J. Heeger (2007). Science 317, 222–225.

[79] H. Ma, H. L. Yip, F. Huang, and A. K.-Y. Jen, (2010). Adv. Funct. Mater. 20, 1371–1388.

[80] Z. He, C. Zhong, S. Su, M. Xu, H. Wu, and Y. Cao (2012). Nat. Photonics 6,591–595.

[81] G. Li, R. Zhu, and Y. Yang (2012). "Polymer solar cells," Nat. Photonics 6, 153–161.

[82] H. Spanggaard and F. C. Krebs (2004). Sol. Energy Mater. Sol. Cells 83, 125–146.

[83] S.-I. Na, S.-S. Kim, J. Jo, and D.-Y. Kim (2008). Adv. Mater. 20, 4061–4067.

[84] Y. J. Cho, J. Y. Lee, B. D. Chin, and S. R. Forrest (2013). Org. Electron. 14, 081–1085.

[85] C. J. Brabec, S. E. Shaheen, C. Winder, N. S. Sariciftci, and P. Denk (2002). Appl. Phys. Lett. 80, 1288–1290.

[86] C. M. Ramsdale, J. A. Barker, A. C. Arias, J. D. MacKenzie, R. H. Friend, and N. C. Greenham (2002). J. Appl. Phys. 92, 4266–4270.

[87] S. Khodabakhsh, B. M. Sanderson, J. Nelson, and T. S. Jones (2006). Adv. Funct. Mater. 16, 95–100.

[88] J. S. Kim, J. H. Park, J. H. Lee, J. Jo, D. Y. Kim, and K. Cho (2007). Appl. Phys. Lett. 91, 112111–112113.

[89] M.-Y. Chang, C.-S. Wu, Y.-F. Chen, B.-Z. Hsieh, W.-Y. Huang, K.-S. Ho, T.-H. Hsieh, and Y.-K. Han, (2008). Org. Electron. 9, 1136–1139.

[90] Sayantan Das and T. L. Alford (2014). Improved efficiency of P3HT:PCBM solar cells by incorporation of silveroxide interfacial layer. Journal Of Applied Physics 116, 044905.